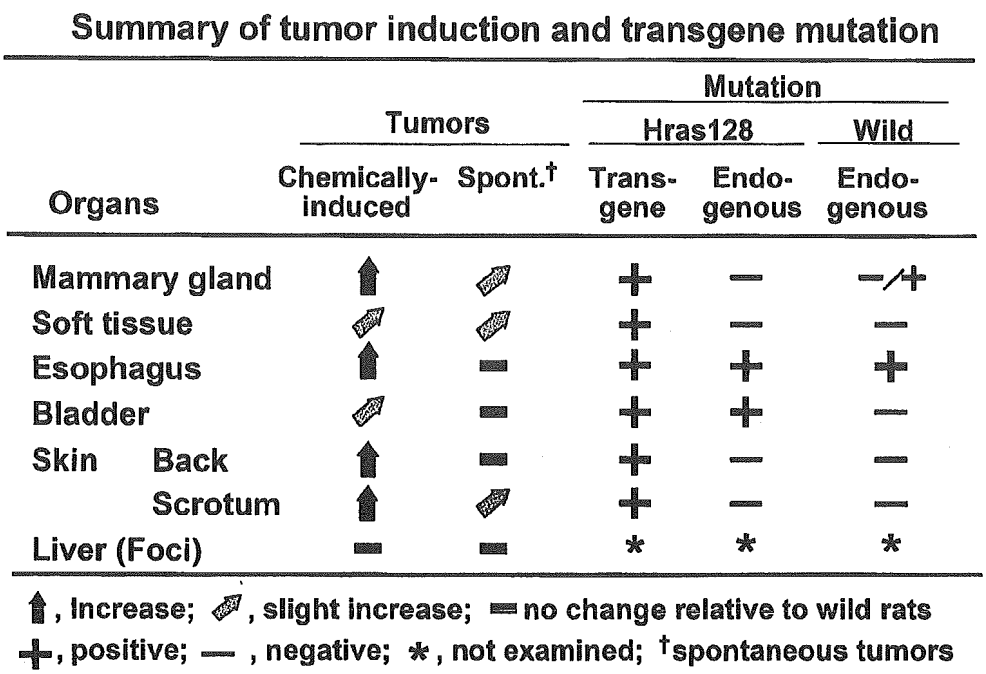

Fig. 5. Summary of data for the organ specificity for susceptibility to tumor induction, transgene mutations and endogenous ras gene mutations.

Other organ carcinogenesis

Skin. We have been able to establish a novel rat skin carcinogenesis model using males of our transgenic strain. Male and female transgenic rats were topically treated with DMBA on the back skin at 50 days after birth, and thereafter were similarly exposed to 2-o-tetradecanoylphorbol 13-acetate (TPA), three times a week for 31 weeks. Squamous cell papillomas and carcinomas, were preferentially induced at the painting sites with DMBA followed by TPA, 100%; DMBA, 75%; TPA, 16.7%. Unexpectedly, a high incidence of skin tumors was also noted on the remote scrotal skin. Furthermore, in females, mammary carcinomas, distant from the painting sites, were primarily induced with a few skin lesions. The results indicate that in addition to mammary cells, epidermal cells are also susceptible to initiation by DMBA.[26]

Urinary bladder. To examine susceptibility to N-butyl-N-(4-hydroxybutyl)nitrosamine (BBN)-induction of urinary bladder carcinogenesis, male transgenic and wild-type littermates were treated with 0.05% BBN in their drinking water for 10 weeks and killed at week 20. The number of bladder tumors, transitional cell papillomas and carcinomas, were greater in the transgenic rats than in their wild-type counterparts. Two cases of transitional cell carcinomas exhibiting invasion of the bladder muscle layer, were also observed to be limited to Hras128 rats. These results indicate that the Hras128 rat is highly susceptible to BBN carcinogenesis and may be used as a rat model for analysis of bladder tumor development.[24]

Esophagus. The transgenic rats were also found to be highly susceptible to N-nitrosomethylbenzylamine induction of esophageal carcinogenesis. Multiple esophageal lesions, squamous cell papillomas and carcinomas, rapidly developed within 10-weeks after application of the carcinogen, at 7-fold the number of tumors found in wild-type rats. Codon 12 GGC to GAC mutations of the transgene were detected at high incidence (76%), along with less frequent mutations of endogenous rat c-Ha-ras gene (8%).[25]

Discussion

Although the human c-Ha-ras proto-oncogene is transduced with its own promoter region, and therefore the gene mRNA is expressed, in all organs, the Hras128 transgenic rat does not exhibit enhanced carcinogenesis independent of the tissue but rather shows organotropic effects (see Fig. 5 for a summary of the findings so far). For example, intestine and prostate tumor induction in male rats was not different from that in wild type littermates after treatment with PhIP.[32] Similarly, no differences were observed in the incidences of liver, lung and thyroid tumors with dihydroxy-*di-n*-propyl nitrosamine. It is interesting that all of the organs that exhibit enhanced susceptibility to carcinogens are known as organs in which endogenous c-Ha-ras gene mutations have been found in chemically induced tumors in wild rats. For example, this is the case in the mammary gland,[48–52] esophagus,[53,54] bladder[55,56] and skin.[57] This is one conceivable reason for the organ-specific predisposition of organotropic oncogenicity with the c-Ha-ras gene (Table 2).

In the mammary gland, the transgene itself appears to increase the number of TEB and enhance proliferation, as evidenced by an increase in activated MAPK and expression of CyclinD2 and D3. Such proliferation-prone conditions are associated with mutations of the transgene in normal-looking endbuds.[40] From our results and the known pathways involving ras (Fig. 6), we speculate that mutated H-ras causes chronic upregulation of signaling through Raf and, therefore, transcription of genes responsible for cell growth. This may correspond to human cases with diseased conditions featuring chronically elevated cell turnover, which may facilitate induction of mutations in cancer related genes, including the ras gene,[58–61] by environmental agents. Actually, enhanced cell proliferation of human mammary tissue cells was shown to be relevant to carcinogenesis.[39,62] Our results may support the hypothesis proposed by Kumar *et al.* that normal physiological proliferative processes can lead to development of carcinomas if the targeted cells harbor latent ras oncogenes under conditions with some stimulus for cell proliferation.[63]

Table 2. Correlation of susceptibility of Hras128 rats to carcinogens and H- or K-ras mutations in tumors in the rat, mouse and human

Tumor site	Enhanced tumor induction in Hras128 rats[1]	H- or K-ras mutation in tumor of		
		Rat	Mouse	Human
Mammary gland	Yes	Hras	Hras	–
Skin	Yes	Hras	Hras	–
Colon	No	Kras	Kras	Kras
Bladder	Yes	–	–	Hras
Pancreas	No	–	–	Kras
Lung	No	Kras	Kras	Kras
Esophagus	Yes	Hras	–	–

[1]As compared to wild-type rats; –, not reported or no mutations found.

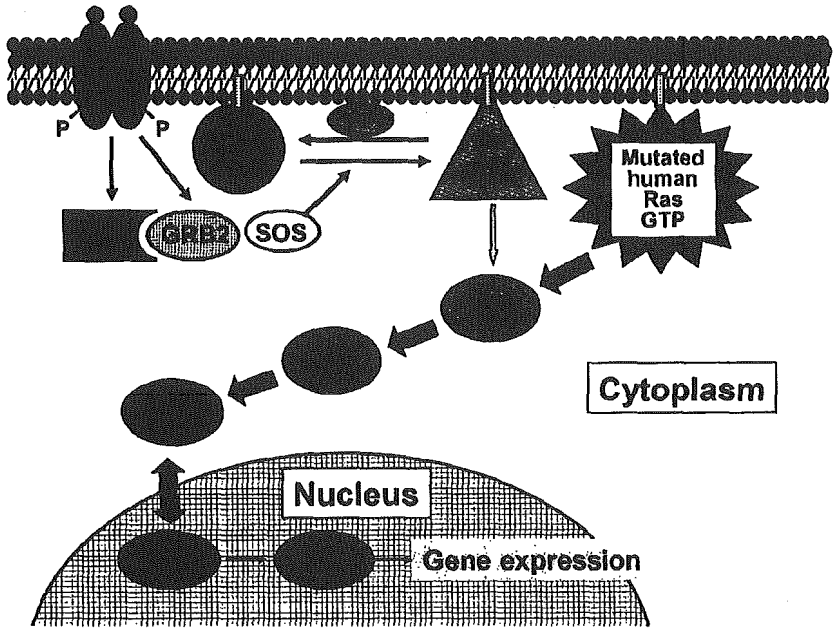

Fig. 6. Schematic presentation of relevant signal pathways in Hras128 rats. The mutated c-Ha-ras oncogene plays a dominant role in activation of the MAPK pathway by binding to Raf.

In addition to mammary carcinogenesis, the Hras128 transgenic rat was found to be susceptible to esophageal and urinary bladder and provides the first rat model featuring rapid generation of skin tumors. The latter has particular advantages in terms of wide application (painting) area and therefore can be used for the testing of compounds for carcinogenicity. For dominant activity in inducing tumors in some limited organs, studies on the possible involvement of some competitive inhibition mechanisms in activation of the ras genc are obviously required.

In conclusion, irrespective of the mechanisms involved in its high susceptibility to chemical carcinogenesis in particular organs, the transgenic rat offers a good model of human mammary carcinogenesis and promising short-term *in vivo* assay model for environmental carcinogens and modifying agents.

Acknowledgments

This study was supported in part by a Grant-in-Aid for the Second Term Comprehensive 10-Year Strategy for Cancer Control, a Grant-in-Aid for Cancer Research (KAKENHI) on Priority Area from the Ministry of Education, Science, Sports, and Culture of Japan, a research grant from the Princess Takamatsu Cancer Research Fund, a Grant-in-Aid for the Foundation for Promotion of Cancer Research in Japan and a Grant-in-Aid from CREST (Core Research for Evolutional Science and Technology) of Japan Science and Technology Corporation (JST), a Grant-in Aid for The Long-range Research Initiative (LRI) from Japan Chemical Industry Association (CC05-01). We also thank Dr Malcolm A. Moore for his kind advice during preparation of the manuscript.

References

1 Usui T, Mutai M, Hisada S *et al.* CB6F1-rasH2 mouse: overview of available data. *Toxicol Pathol* 2001; **29** (Suppl.): 90–108.
2 Tamaoki N. The rasH2 transgenic mouse: nature of the model and mechanistic studies on tumorigenesis. *Toxicol Pathol* 2001; **29** (Suppl.): 81–9.
3 Ando K, Saitoh A, Hino O, Takahashi R, Kimura M, Katsuki M. Chemically induced forestomach papillomas in transgenic mice carry mutant human c-Ha-ras transgenes. *Cancer Res* 1992; **52**: 978–82.
4 Tennant RW, Stasiewicz S, Eastin WC, Mennear JH, Spalding JW. The Tg.AC (v-Ha-ras) transgenic mouse: nature of the model. *Toxicol Pathol* 2001; **29** (Suppl.): 51–9.
5 Spalding JW, Momma J, Elwell MR, Tennant RW. Chemically induced skin carcinogenesis in a transgenic mouse line (Tg.AC) carrying a v-Ha-ras gene. *Carcinogenesis* 1993; **14**: 1335–41.
6 Breuer M, Slebos R, Verbeek S, van Lohuizen M, Wientjens E, Berns A. Very high frequency of lymphoma induction by a chemical carcinogen in pim-1 transgenic mice. *Nature* 1989; **340**: 61–3.

 doi: 10.1111/j.1349-7006.2005.00056.x

7 Storer RD, Cartwright ME, Cook WO, Soper KA, Nichols WW. Short-term carcinogenesis bioassay of genotoxic procarcinogens in PIM transgenic mice. *Carcinogenesis* 1995; **16**: 285–93.
8 Hully JR, Su Y, Lohse JK *et al.* Transgenic hepatocarcinogenesis in the rat. *Am J Pathol* 1994; **145**: 386–97.
9 Tsuda H, Asamoto M, Baba H *et al.* Cell proliferation and advancement of hepatocarcinogenesis in the rat are associated with a decrease in connexin 32 expression. *Carcinogenesis* 1995; **16**: 101–5.
10 Tsuda H, Ozaki K, Uwagawa S *et al.* Effects of modifying agents on conformity of enzyme phenotype and proliferative potential in focal preneoplastic and neoplastic liver cell lesions in rats. *Jpn J Cancer Res* 1992; **83**: 1154–65.
11 Dragan YP, Peterson J, Pitot HC. Comparison of hepatocyte phenotypes at the glutathione transferase and albumin loci in Sprague-Dawley and Nagase analbuminemic rats and F1 progeny after initiation and promotion. *Carcinogenesis* 1993; **14**: 1313–9.
12 Asamoto M, Hokaiwado N, Cho YM *et al.* Prostate carcinomas developing in transgenic rats with SV40 T antigen expression under probasin promoter control are strictly androgen dependent. *Cancer Res* 2001; **61**: 4693–700.
13 Asamoto M, Hokaiwado N, Cho YM, Shirai T. Effects of genetic background on prostate and taste bud carcinogenesis due to SV40 T antigen expression under probasin gene promoter control. *Carcinogenesis* 2002; **23**: 463–7.
14 Haas MJ, Pitot HC. Characterization of rare p53 mutants from carcinogen-treated albumin-simian virus 40 T-antigen transgenic rats. *Mol Carcinog* 1998; **21**: 128–34.
15 Dragan YP, Sargent LM, Babcock K, Kinunen N, Pitot HC. Alterations in specific gene expression and focal neoplastic growth during spontaneous hepatocarcinogenesis in albumin-SV40 T antigen transgenic rats. *Mol Carcinog* 2004; **40**: 150–9.
16 Haas MJ, Sattler CA, Dragan YP, Gast WL, Pitot HC. Multiple polypeptide hormone expression in pancreatic islet cell carcinomas derived from phosphoenolpyruvatecarboxykinase-SV40 T antigen transgenic rats. *Pancreas* 2000; **20**: 206–14.
17 Davies BR, Platt-Higgins AM, Schmidt G, Rudland PS. Development of hyperplasias, preneoplasias, and mammary tumors in MMTV-c-erbB-2 and MMTV-TGFalpha transgenic rats. *Am J Pathol* 1999; **155**: 303–14.
18 Watson PA, Kim K, Chen KS, Gould MN. Androgen-dependent mammary carcinogenesis in rats transgenic for the Neu proto-oncogene. *Cancer Cell* 2002; **2**: 67–79.
19 Nakae D, Denda A, Kobayashi Y *et al.* Inhibition of early-phase exogenous and endogenous liver carcinogenesis in transgenic rats harboring a rat glutathione S-transferase placental form gene. *Jpn J Cancer Res* 1998; **89**: 1118–25.
20 Kobayashi T, Mitani H, Takahashi R *et al.* Transgenic rescue from embryonic lethality and renal carcinogenesis in the Eker rat model by introduction of a wild-type Tsc2 gene. *Proc Natl Acad Sci USA* 1997; **94**: 3990–3.
21 Momose S, Kobayashi T, Mitani H *et al.* Identification of the coding sequences responsible for Tsc2-mediated tumor suppression using a transgenic rat system. *Hum Mol Genet* 2002; **11**: 2997–3006.
22 Haas MJ, Dragan YP, Hikita H *et al.* Transgene expression and repression in transgenic rats bearing the phosphoenolpyruvate carboxykinase-simian virus 40 T antigen or the phosphoenolpyruvate carboxykinase-transforming growth factor-alpha constructs. *Am J Pathol* 1999; **155**: 183–92.
23 Asamoto M, Ochiya T, Toriyama-Baba H *et al.* Transgenic rats carrying human c-Ha-ras proto-oncogenes are highly susceptible to N-methyl-N-nitrosourea mammary carcinogenesis. *Carcinogenesis* 2000; **21**: 243–9.
24 Ota T, Asamoto M, Toriyama-Baba H *et al.* Transgenic rats carrying copies of the human c-Ha-ras proto-oncogene exhibit enhanced susceptibility to N-butyl-N-(4-hydroxybutyl) nitrosamine bladder carcinogenesis. *Carcinogenesis* 2000; **21**: 1391–6.
25 Asamoto M, Toriyama-Baba H, Ohnishi T *et al.* Transgenic rats carrying human c-Ha-ras proto-oncogene are highly susceptible to N-nitrosomethylbenzylamine induction of esophageal tumorigenesis. *Jpn J Cancer Res* 2002; **93**: 744–51.
26 Park CB, Fukamachi K, Takasuka N *et al.* Rapid induction of skin and mammary tumors in human c-Ha-ras proto-oncogene transgenic rats by treatment with 7,12-dimethylbenz[a]anthracene followed by 12-O-tetradecanoylphorbol 13-acetate. *Cancer Sci* 2004; **95**: 205–10.
27 Kikuchi K, Ikeda H, Tsuchikawa T *et al.* A novel animal model of thymic tumour: development of epithelial thymoma in transgenic rats carrying human T lymphocyte virus type I pX gene. *Int J Exp Pathol* 2002; **83**: 247–55.
28 Hammer RE, Richardson JA, Simmons WA, White AL, Breban M, Taurog JD. High prevalence of colorectal cancer in HLA-B27 transgenic F344 rats with chronic inflammatory bowel disease. *J Investig Med* 1995; **43**: 262–8.
29 Thompson TA, Haag JD, Lindstrom MJ, Griep AE, Lohse JK, Gould MN. Decreased susceptibility to NMU-induced mammary carcinogenesis in transgenic rats carrying multiple copies of a rat ras gene driven by the rat Harvey ras promoter. *Oncogene* 2002; **21**: 2797–804.
30 Tsuda H, Asamoto M, Ochiya T *et al.* High susceptibility of transgenic rats carrying the human c-Ha-ras proto-oncogene to chemically-induced mammary carcinogenesis. *Mutat Res* 2001; **477**: 173–82.
31 Sekiya T, Fushimi M, Hori H, Hirohashi S, Nishimura S, Sugimura T. Molecular cloning and the total nucleotide sequence of the human c-Ha-ras-1 gene activated in a melanoma from a Japanese patient. *Proc Natl Acad Sci USA* 1984; **81**: 4771–5.
32 Naito A, Suzuki A, Ueda S *et al.* Preferential mammary carcinogenic effects of 2-amino-1-methyl-6-phenylimidazo[4,5-b]pyridine (PhIP) in human c-Ha-ras proto-oncogene transgenic rats. *Cancer Sci* 2004; **95**: 399–403.
33 Costa I, Solanas M, Escrich E. Histopathologic characterization of mammary neoplastic lesions induced with 7,12 dimethylbenz (alpha) anthracene in the rat: a comparative analysis with human breast tumors. *Arch Pathol Laboratory Med* 2002; **126**: 915–27.
34 Russo J, Russo IH. Atlas and histologic classification of tumors of the rat mammary gland. *J Mammary Gland Biol Neoplasia* 2000; **5**: 187–200.
35 Zhang LH, Jenssen D. Site specificity of N-methyl-N-nitrosourea-induced transition mutations in the hprt gene. *Carcinogenesis* 1991; **12**: 1903–9.
36 Ip C, Daniel FB. Effects of selenium on 7,12-dimethylbenz(a) anthracene-induced mammary carcinogenesis and DNA adduct formation. *Cancer Res* 1985; **45**: 61–5.
37 Nagao M, Ushijima T, Toyota M, Inoue R, Sugimura T. Genetic changes induced by heterocyclic amines. *Mutat Res* 1997; **376**: 161–7.
38 Asamoto M, Ota T, Toriyama-Baba H, Hokaiwado N, Naito A, Tsuda H. Mammary carcinomas induced in human c-Ha-ras proto-oncogene transgenic rats are estrogen-independent, but responsive to d-limonene treatment. *Jpn J Cancer Res* 2002; **93**: 32–5.
39 Russo J, Russo IH. Experimentally induced mammary tumors in rats. *Breast Cancer Res Treat* 1996; **39**: 7–20.
40 Hamaguchi T, Matsuoka Y, Kawaguchi H *et al.* Terminal endbuds and acini as the respective major targets for chemical and sporadic carcinogenesis in the mammary glands of human c-Ha-ras protooncogene transgenic rats. *Breast Cancer Res Treat* 2004; **83**: 43–56.
41 Thompson HJ, Singh M. Rat models of premalignant breast disease. *J Mammary Gland Biol Neoplasia* 2000; **5**: 409–20.
42 Shilkaitis A, Green A, Steele V, Lubet R, Kelloff G, Christov K. Neoplastic transformation of mammary epithelial cells in rats is associated with decreased apoptotic cell death. *Carcinogenesis* 2000; **21**: 227–33.
43 Matsuoka Y, Fukamachi K, Hamaguchi T *et al.* Rapid emergence of mammary preneoplastic and malignant lesions in human c-Ha-ras proto-oncogene transgenic rats: possible application for screening of chemopreventive agents. *Toxicol Pathol* 2003; **31**: 632–7.
44 Fukamachi K, Matsuoka Y, Kitanaka C, Kuchino Y, Tsuda H. Rat neuronal leucine-rich repeat protein-3: cloning and regulation of the gene expression. *Biochem Biophys Res Commun* 2001; **287**: 257–63.
45 Fukamachi K, Matsuoka Y, Ohno H, Hamaguchi T, Tsuda H. Neuronal leucine-rich repeat protein-3 amplifies MAPK activation by epidermal growth factor through a carboxyl-terminal region containing endocytosis motifs. *J Biol Chem* 2002; **277**: 43549–52.
46 Han BS, Fukamachi K, Takasuka N *et al.* Inhibitory effects of 17beta-estradiol and 4-n-octylphenol on 7,12-dimethylbenz[a]anthracene-induced mammary tumor development in human c-Ha-ras proto-oncogene transgenic rats. *Carcinogenesis* 2002; **23**: 1209–15.
47 Fukamachi K, Han BS, Kim CK *et al.* Possible enhancing effects of atrazine and nonylphenol on 7,12-dimethylbenz[a]anthracene-induced mammary tumor development in human c-Ha-ras proto-oncogene transgenic rats. *Cancer Sci* 2004; **95**: 404–10.
48 Yu M, Snyderwine EG. H-ras oncogene mutations during development of 2-amino-1-methyl-6-phenylimidazo[4,5-b]pyridine (PhIP)-induced rat mammary gland cancer. *Carcinogenesis* 2002; **23**: 2123–8.
49 Ushijima T, Makino H, Kakiuchi H, Inoue R, Sugimura T, Nagao M. Genetic alterations in HCA-induced tumors. *Princess Takamatsu Symp* 1995; **23**: 281–91.
50 Sukumar S, McKenzie K, Chen Y. Animal models for breast cancer. *Mutat Res* 1995; **333**: 37–44.
51 Shirai K, Uemura Y, Fukumoto M *et al.* Synergistic effect of MNU and DMBA in mammary carcinogenesis and H-ras activation in female Sprague-Dawley rats. *Cancer Lett* 1997; **120**: 87–93.
52 Hokaiwado N, Asamoto M, Cho YM, Imaida K, Shirai T. Frequent c-Ha-ras gene mutations in rat mammary carcinomas induced by 2-amino-1-methyl-6-phenylimidazo[4,5-b]pyridine. *Cancer Lett* 2001; **163**: 187–90.
53 Fong LY, Lau KM, Huebner K, Magee PN. Induction of esophageal tumors in zinc-deficient rats by single low doses of N-nitrosomethylbenzylamine (NMBA): analysis of cell proliferation, and mutations in H-ras and p53 genes. *Carcinogenesis* 1997; **18**: 1477–84.
54 Liston BW, Gupta A, Nines R *et al.* Incidence and effects of Ha-ras codon 12 G → A transition mutations in preneoplastic lesions induced by

N-nitrosomethylbenzylamine in the rat esophagus. *Mol Carcinog* 2001; **32**: 1–8.
55 Masui T, Shirai T, Imaida K *et al.* Ki-ras mutations with frequent normal allele loss versus absence of p53 mutations in rat prostate and seminal vesicle carcinomas induced with 3,2′-dimethyl-4-aminobiphenyl. *Mol Carcinog* 1995; **13**: 21–6.
56 Jones RF, Debiec-Rychter M, Zukowski K, Wang CY. Activating missense mutations in IIa-ras-1 genes in a malignant subset of bladder lesions induced by N-butyl-N-(4-hydroxybutyl) nitrosamine or N-[4-(5-nitro-2-furanyl)-2-thiazolyl]formamide. *Mol Carcinog* 1990; **3**: 393–402.
57 Ronai ZA, Gradia S, el-Bayoumy K, Amin S, Hecht SS. Contrasting incidence of ras mutations in rat mammary and mouse skin tumors induced by anti-benzo[c]phenanthrene-3,4-diol-1,2-epoxide. *Carcinogenesis* 1994; **15**: 2113–6.
58 Bos JL. Ras oncogenes in human cancer: a review. *Cancer Res* 1989; **49**: 4682–9.
59 Schwartz L, Balosso J, Baillet F, Brun B, Amman JP, Sasco AJ. Cancer: the role of extracellular disease. *Med Hypotheses* 2002; **58**: 340–6.
60 Johansson SL, Anderstrom C, von Schultz L, Larsson P. Enhancement of N-[4-(5-nitro-2-furyl)-2-thiazolyl]formamide-induced carcinogenesis by urinary tract infection in rats. *Cancer Res* 1987; **47**: 559–62.
61 Correa P. The biological model of gastric carcinogenesis. *IARC Sci Publ* 2004: 301–10.
62 Gaglia P, Bernardi A, Venesio T *et al.* Cell proliferation of breast cancer evaluated by anti-BrdU and anti-Ki-67 antibodies: its prognostic value on short-term recurrences. *Eur J Cancer* 1993; **29A**: 1509–13.
63 Kumar R, Sukumar S, Barbacid M. Activation of ras oncogenes preceding the onset of neoplasia. *Science* 1990; **248**: 1101–4.

 doi: 10.1111/j.1349-7006.2005.00056.x

16

Dietary Supplementation with Silymarin Inhibits 3,2'-Dimethyl-4-Aminobiphenyl–Induced Prostate Carcinogenesis in Male F344 Rats

Hiroyuki Kohno,[1] Rikako Suzuki,[1] Shigeyuki Sugie,[1] Hiroyuki Tsuda,[2] and Takuji Tanaka[1]

Abstract **Purpose:** Silymarin has been shown to be a potent anticarcinogenic agent. Here, we investigated the modifying effects of dietary feeding with a naturally occurring polyphenolic antioxidant flavonoid silymarin on 3,2'-dimethyl-4-aminobiphenyl (DMAB)–induced prostatic carcinogenesis in male F344 rats.

Experimental Design: Male F344 rats were given s.c. injections of DMAB (25 mg/kg body weight) every other week for 20 weeks. They also received the experimental diet containing 100 or 500 ppm silymarin for 40 weeks, starting 1 week after the last dosing of DMAB. All of the rats were sacrificed 60 weeks after the start of the experiment. Histopathology and immunohistochemistry for proliferative cell nuclear antigen, cyclin D1, and apoptotic indices were done in the prostatic lesions, including invasive adenocarcinomas, intraepithelial neoplasms, and nonlesional glands.

Results: Dietary feeding with 500 ppm silymarin significantly inhibited the incidence of prostatic adenocarcinoma when compared with the DMAB-alone group (17.6% versus 50.0%, $P < 0.05$). The proliferative cell nuclear antigen– and cyclin D1–positive indices in adenocarcinomas, prostatic intraepithelial neoplasm, and nonlesional glands in rats treated with DMAB and silymarin were slightly lower than that of the DMAB-alone group. Also, dietary administration of silymarin increased apoptotic index in prostatic adenocarcinoma by measuring immunohistochemically positive nuclei for ssDNA.

Conclusions: Our results indicate that silymarin exerts chemopreventive ability against chemically induced prostatic carcinogenesis through apoptosis induction and modification of cell proliferation.

Prostate cancer is the most common type of cancer found in older men and the leading cause of cancer mortality in men (1). In Japan, the incidence and mortality rates of this malignancy are lower compared with Western populations (2), but they have gradually increased (3). Furthermore, migrant studies have shown that the incidence of prostate cancer increases generation by generation after immigration in Japanese-Americans (4). These observations strongly suggest that the wide disparity in prostate cancer incidence worldwide is attributable to dietary habits, among which are a regimen rich in several flavonoids and isoflavones that inhibits the progression of prostate cancer by modulating epigenetic events (5). It is, therefore, necessary to intensify our efforts to better understand this disease and develop novel approaches for its prevention and treatment.

Silymarin, the collective name for an extract from the milk thistle [*Silybum marianum* (L.) Gaertneri], is a naturally occurring polyphenolic flavonoid antioxidant. It is composed mainly of silibinin (~80%, w/w; also called silybin, silibin, or sibilinin) with smaller amounts of other stereoisomers (isosilybin, dihydrosibilyn, silydianin, and silychristin, etc.; ref. 6). Silymarin has strong antioxidative properties and is able to scavenge both free radicals and reactive oxygen species (7, 8). In Europe, for over 20 years, silymarin, as an antihepatotoxic, is used clinically for the treatment of alcoholic liver disease (9, 10). In recent years, silymarin has also been used in Asia as a therapeutic agent for liver diseases (6). Silymarin is well tolerated and largely free of adverse effects (6, 11). Silymarin acts as a potent anticarcinogenic agent against *in vitro* and *in vivo* carcinogenesis experiments (12–14). Silymarin and silibinin, which is the major active constituent of silymarin, can inhibit the growth of human prostate carcinoma LNCaP, PC-3, and DU145 cells in culture (15–17). Moreover, silymarin and

Authors' Affiliations: [1]Department of Oncologic Pathology, Kanazawa Medical University, Ishikawa, Japan and [2]Department of Molecular Toxicology, Nagoya City University Graduate School of Medical Sciences, Nagoya, Japan

Received 1/19/05; revised 3/31/05; accepted 4/6/05.

Grant support: Grant-in-Aid (13-15) for Cancer Research from the Ministry of Health, Labour and Welfare of Japan; Grant-in-Aid for the third term for a Comprehensive 10-Year Strategy for Cancer Control from the Ministry of Health, Labour and Welfare of Japan; Grants-in-Aid for Scientific Research from the Ministry of Education, Culture, Sports, Science and Technology of Japan; grant C2004-4 for the Collaborative Research from Kanazawa Medical University; and grant H2004-6 for the Project Research from the High-Technology Center of Kanazawa Medical University.

The costs of publication of this article were defrayed in part by the payment of page charges. This article must therefore be hereby marked *advertisement* in accordance with 18 U.S.C. Section 1734 solely to indicate this fact.

Requests for reprints: Hiroyuki Kohno, Department of Oncologic Pathology, Kanazawa Medical University, 1-1 Daigaku, Uchinada, 920-0293 Ishikawa, Japan. Phone: 81-76-286-2211; Fax: 81-76-286-6926; E-mail: h-kohno@kanazawa-med.ac.jp.

silibinin inhibit cell growth and induce apoptosis in rat prostate cancer cell lines (18). However, chemoprevention studies using silymarin in rodent were limited to skin (13, 19). Silymarin inhibits tumor promoter-caused induction of ornithine decarboxylase activity and mRNA expression in mouse epidermis (20). Silymarin inhibits mRNA expression of endogenous tumor promoter tumor necrosis factor-α (21). More recently, silymarin has been reported to inhibit activation of erbB1 signaling, induce cyclin-dependent kinase inhibitors, G_1 arrest, and cause complete inhibition of growth of human prostate carcinoma DU145 cells (17). Also, silymarin, at lower nontoxic concentrations, can inhibit transformation in cultured rat tracheal epithelial cells treated with benzo(*a*)pyrene (22). These findings led us to evaluate the possible suppressing effects of dietary silymarin on the occurrence of chemically induced neoplasms in organs other than skin of rodents. We recently have found the inhibitory effects of dietary administration of silymarin against rat tongue (23), mouse urinary bladder (24), and rat colon (25) carcinogenesis.

In the current study, we investigated the effects of silymarin on 3,2′-dimethyl-4-aminobiphenyl (DMAB)-initiated prostate carcinogenesis in male F344 rats. Also, the modulatory effects of the silymarin on the proliferating cell nuclear antigen (PCNA), cyclin D1, and apoptotic indices were immunohitochemically investigated in the prostatic lesions induced by DMAB.

Materials and Methods

Animals, chemicals, and diets. Four-week-old male F344 rats (Charles River Japan, Inc., Kanagawa, Japan) were used. The animals were maintained in the Kanazawa Medical University Animal Facility according to the Institutional Animal Care Guidelines. All animals were housed in polycarbonate cages (three or four rats per cage) under controlled conditions of humidity (50 ± 10%), lighting (12-hour light/dark cycle), and temperature (23 ± 2°C). They have free access to drinking water (ion exchange water) and a basal diet, CRF-1 (Oriental Yeast, Co., Ltd., Tokyo, Japan) from which soy constituents were eliminated throughout the study. Animals were quarantined for 7 days and randomized by body weight into experimental and control groups. DMAB and silymarin were obtained from Sigma-Aldrich Japan, K.K. (Tokyo, Japan). The experimental diet containing silymarin were prepared by Oriental Yeast by adding test chemicals to soy protein-free CRF-1.

Experimental procedure. A total of 68 male F344 rats were divided into nine experimental and control groups. The animals in groups 1 through 3 were given DMAB dissolved in DMSO, s.c., at a dose of 25 mg/kg body weight every other week for 20 weeks. DMAB injection was done between 10:00 a.m. and 11:00 a.m. From 1 week after the last injection of DMAB, group 1 was given the basal diet without silymarin, groups 2 and 3 received silymarin-containing diets (100 ppm for group 2 and 500 ppm for group 3), and group 4 was fed the diet containing 500 ppm silymarin for 40 weeks. Group 5 served as an untreated control. The doses of the test compounds were selected based on previous studies (23). All rats were sacrificed at week 60 by ether overdose to assess the pathologic lesions in all organs, including prostate. At autopsy, all organs were carefully inspected and all macroscopic pathologic findings were recorded. All grossly abnormal lesions in any tissue and the organs, such as accessory sex organs including prostate, liver, kidney, lung, and heart, were fixed in 10% phosphate-buffered formalin for 2 weeks. As for the accessory sex organs, two sagittal slices of the ventral prostate, two sagittal slices of the dorsolateral prostate, which included the urethra, and three transverse slices from each side of the seminal vesicles, which included the anterior prostate, were made and embedded in paraffin. They were then sectioned and stained with H&E for histopathologic diagnosis. The prostatic lesions, including prostatic intraepithelial neoplasm (PIN; ref. 26), were histopathologically diagnosed. The diagnosis of PIN was based on the criteria described by Bostwick and Brawer (27): PIN shows the morphologic continuum of cellular proliferations with nuclear atypia that occur within prostatic ducts, ductules, or acini, and is enclosed by a basement membrane. Several architectural patterns, such as flat, tufting, microcapillary, or cribriform, could be seen.

Immunohistochemistry. For the determination of cell proliferation and cell cycle activity of the epithelial cells, PCNA and cyclin D1 immunohistochemistry was done according to the method described previously with some modifications (28, 29). Apoptotic index was also evaluated by immunohistochemistry for ssDNA (28). Immunohistochemistry was done using a stain system kit (DAKO LSAB 2 kit/HRP, DAKO Japan Co., Ltd., Kyoto, Japan). The sections (3 μm in thickness) made from paraffin-embedded tissues were deparaffinized; they were treated sequentially with 0.3% H_2O_2, normal goat serum or horse serum, and first antibodies. A mouse anti-PCNA antibody (1:100 dilution; DAKO Japan), a rabbit polyclonal anti-cyclin D1 antibody (1:3,000 dilution; Santa Cruz Biotechnology, Santa Cruz, CA), and a rabbit polyclonal antibody against ssDNA (1:300; DAKO Japan) were applied to the sections according to the manufacturer's protocol (DAKO LSAB 2 kit/HRP, DAKO Japan). All incubation steps ware carried out for 15 minutes at 37°C. The chromogen used was 3,3′-diaminobenzidine tetrahydrochloride. The tissues were lightly counterstained with hematoxylin to facilitate orientation. Negative controls were stained without the first antibodies. The numbers of cells with positive reactivity for PCNA, cyclin D1, and ssDNA antibody were counted in a total of 3 × 100 cells in three different areas of the tumors, PIN, and nonlesional areas, and expressed as percentage (mean ± SD).

Statistical evaluation. Where applicable, data were analyzed using Fisher's exact probability test, Student's *t* test, or Welch *t* test with $P < 0.05$ as the criterion of significance.

Table 1. Intakes of food and test chemical

Group no.	Treatment	No. rats examined	Daily intake		Total intake of test chemical (mg)
			Food (g/d/rat)	Test chemical (mg/d/rat)	
1	DMAB	18	16.1 ± 2.5*	—	—
2	DMAB → 100 ppm silymarin	17	16.0 ± 2.6	1.60	44.8
3	DMAB → 500 ppm silymarin	17	16.4 ± 2.3	8.20	2,296
4	500 ppm silymarin	8	16.3 ± 2.2	8.15	2,282
5	None	8	15.8 ± 1.7	—	—

*Mean ± SD.

Table 2. Body, liver, prostate, and testicular weights at the end of the study

Group no.	Treatment	No. rats examined	Body weight (g)	Liver weight (g)	Prostate weight (g)	Testes weight (g)
1	DMAB	18	384.8 ± 24.4*	11.82 ± 1.25	3.19 ± 0.61	2.88 ± 0.66
2	DMAB → 100 ppm silymarin	17	386.0 ± 21.3	12.30 ± 0.93	3.18 ± 0.59	2.80 ± 0.55
3	DMAB → 500 ppm silymarin	17	388.7 ± 16.1	12.42 ± 1.00	3.13 ± 0.67	2.79 ± 0.48
4	500 ppm silymarin	8	401.1 ± 11.8	11.76 ± 1.16	3.13 ± 0.45	2.98 ± 0.64
5	None	8	383.9 ± 20.9	12.42 ± 1.19	3.20 ± 0.62	3.03 ± 0.37

*Means ± SD.

Results

General observation. All animals remained healthy throughout the experimental period. During the study, no clinical signs of toxicity were present in any groups. Histologically, there were no pathologic alteration suggesting toxicity of silymarin in the liver, kidneys, lung, and heart. Food consumption (g/d/rat) did not significantly differ among the groups, as shown in Table 1. Estimated intakes of test chemicals were well correlated with doses applied (Table 1). Body, liver, prostate, and testicular weights in all groups at the end of the study are shown in Table 2. The mean body weights, liver, prostate, and bilateral testicular weights did not significantly differ among the groups.

Incidence of neoplasms of prostate and other organs. Table 3 summarizes the data on the incidence of neoplasms of prostate and other tissues. DMAB exposure could induce PIN and adenocarcinomas (Fig. 1A and B) in the ventral lobe of the prostate. Such lesions were not found in other lobes of the prostate and seminal vesicle. Treatment of DMAB alone (group 1) produced 50.0% incidence of well-differentiated prostatic adenocarcinoma (Fig. 1A). The incidence of prostatic adenocarcinoma (Fig. 1B) in group 3 that received DMAB and 500 ppm silymarin (17.6%) was significantly lower than in group 1 (50.0%, $P < 0.05$). Also, feeding with 100 ppm silymarin after DMAB administration (group 2) caused a reduction of incidence of prostatic adenocarcinoma (29.4%), but there was no statistical significance different from group 1. The incidences of prostatic PIN were 50.0% in group 1, 23.5% in group 2, and 64.7% in group 3. These values also did not show statistically significance among the groups 1 through 3. In other organs, a few neoplasms, such as colonic adenocarcinoma, s.c. malignant fibrous histiocytoma, and ear duct squamous cell carcinoma, were noted in a few rats of groups 1 to 3. The incidences of these tumors were not statistically significant among the groups. No prostatic neoplasms were found in groups 4 (500 ppm silymarin alone) and 5 (no treatment).

Immunohistochemical findings. The data on PCNA- (Fig. 1C and D), cyclin D1- (Fig. 1E and F), and apoptosis-positive cells (Fig. 1G and H) in the prostatic lesions are indicated in Table 4. The mean PCNA labeling indices of adenocarcinoma found in group 3 receiving DMAB and 500 ppm silymarin (6.3 ± 1.5) were significantly lower than in group 1 (10.0 ± 2.4, $P < 0.05$). The PCNA labeling indices of PIN in groups 2 (6.8 ± 1.7) and 3 (6.8 ± 2.2) were lower than that of group 1 (8.8 ± 2.9), but the differences were not statistically significant. As for the histologically normal prostatic glands, the PCNA-labeling indices of all groups were comparable. The mean cyclin D1 labeling indices of adenocarcinoma found in groups 2 and 3 were significantly lower than in group 1 ($P < 0.05$ or $P < 0.01$). The cyclin D1 labeling indices of PIN in groups 2 and 3 were slightly lower than that of group 1, but the differences were not statistically significant. As for the histologically normal prostatic glands, the cyclin D1 labeling indices of all groups were comparable. The apoptotic index of PIN and adenocarcinoma in group 3 was statistically greater than that of group 1 ($P < 0.05$ and $P < 0.02$, respectively). On the other hand, the apoptotic index of PIN and adenocarcinoma

Table 3. Incidence of pathologic lesions

Group no.	Treatment	No. rats examined	No. rats with incidence		
			Prostate		Others*
			PIN	Adenocarcinoma	
1	DMAB	18	9 (50.0%)	9 (50%)	4 (22.2%)
2	DMAB → 100 ppm silymarin	17	4 (23.5%)	5 (29.4%)	4 (23.5%)
3	DMAB → 500 ppm silymarin	17	11 (64.7%)	3† (17.6%)	2 (11.8%)
4	500 ppm silymarin	8	0 (0%)	0 (0%)	0 (0%)
5	None	8	0 (0%)	0 (0%)	0 (0%)

*Colonic adenocarcinoma, s.c. malignant fibrous histiocytoma, and ear duct squamous cell carcinoma.
†Significantly different from group 1 by Fisher's exact probability test ($P < 0.05$).

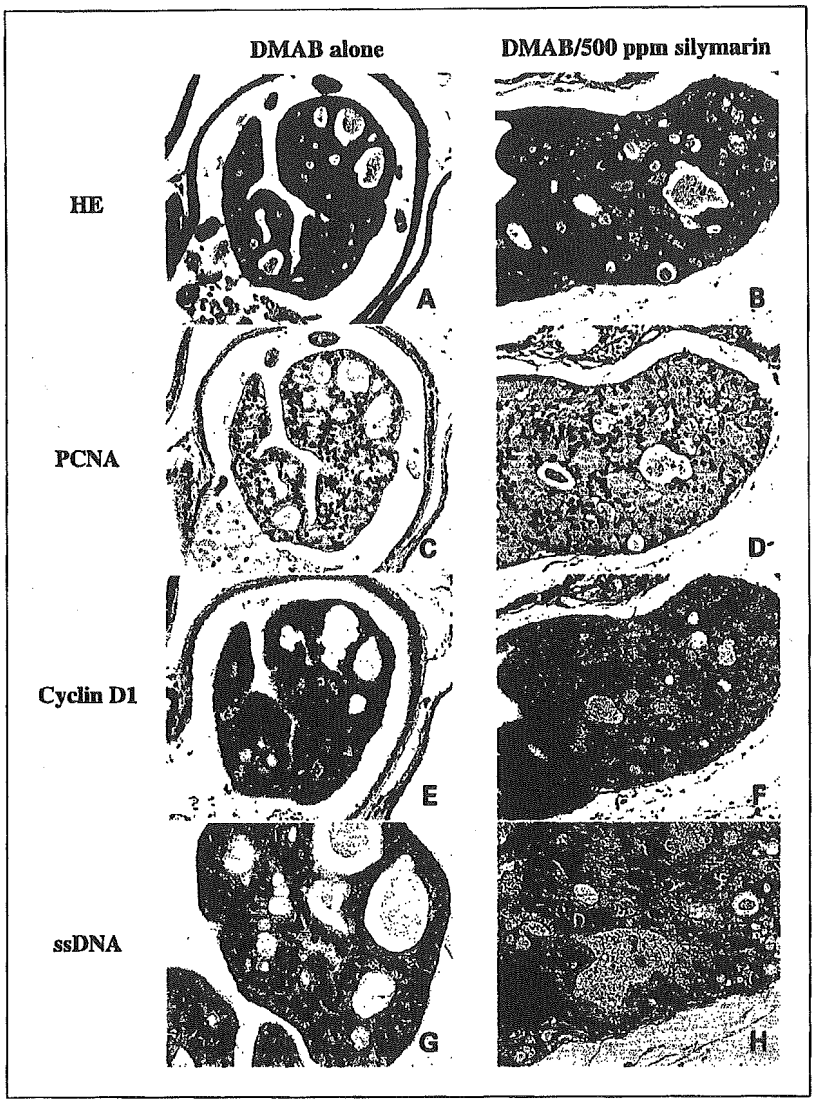

Fig. 1. Histopathology of adenocarcinomas and their immunohistochemistry of PCNA, cyclin D1, and ss DNA. An adenocarcinoma (*A, C, E, G*) from a rat given DMAB alone (group 1) and that (*B, D, F, H*) from a rat given DMAB and 500 ppm silymarin (group 3). H&E stain (*A, B*) and immunohistochemistry for PCNA (*C, D*), cyclin D1 (*E, F*), and ssDNA (*G, H*). Original magnification, ×20 (*A-F*) and ×40 (*G, H*).

in group 2 was lower than that of group 1, but the differences were not statistically significant. As for the histologically normal prostatic glands, the apoptotic indices of all groups were comparable.

Discussion

In the present study, dietary administration of 500 ppm silymarin during the promotion phase of DMAB-induced prostatic carcinogenesis significantly inhibited the incidence of prostatic adenocarcinoma. Silymarin is known to inhibit chemically induced carcinogenesis in skin (13), tongue (23), urinary bladder (24), and colon (25). Furthermore, Singh et al. (30) reported that the preventive and therapeutic efficacy of dietary feeding of silibinin on human prostate carcinoma DU145 tumor xenograft in athymic nude mice. These results indicate that silymarin might be a candidate chemopreventive agent against carcinogenesis in multiple organs including prostate.

Several mechanisms by which chemopreventive agents exert their inhibitory effects on tumorigenesis could be considered. Cell proliferation plays an important role in multistage carcinogenesis and involves multiple genetic alterations (31, 32). Silymarin and silibinin are reported to suppress the growth of different cancer cells (17, 33–35). Other studies with human prostate cancer cells showed that silymarin and silibinin inhibit the cell growth of androgen-dependent and androgen-independent human prostate carcinomas LNCaP and DU145 cells, respectively (15, 17). Tyagi et al. (18) showed that silymarin and silibinin induce growth inhibition and apoptotic cell death in rat prostate cancer cells. Such effects are considered to occur through perturbation of cell cycle progression, leading to G_1 arrest in a dose- and time-dependent manner, and inhibiting DNA synthesis, possibly because of an effect of G_1 arrest (17, 33, 36, 37). Cyclin D1 is involved in cell cycle during early G_1 phase (38). As the major events leading to cell proliferation occur in the G_1 phase, altered expression of cyclin D1 and their cyclin-dependent kinases might be an important step in carcinogenesis (39). Cyclin D1 overexpression was reported in human cancers (40, 41) and in murine chemically induced carcinogenesis (24, 42). Cyclin D1, which is found to be overexpressed in major of human cancers, has been regarded as a

Table 4. PCNA labeling index, cyclin D1–positive index, and apoptotic index in the prostatic lesions

Group no.	Treatment	PCNA labeling index (%)			Cyclin D1 positive index (%)			Apoptotic index (%)		
		PIN	ADC	Nonlesional area	PIN	ADC	Nonlesional area	PIN	ADC	Nonlesional area
1	DMAB	8.8 ± 2.9* (9)	10.0 ± 2.4 (9)	4.6 ± 1.5 (5)	28.4 ± 7.2 (9)	35.7 ± 6.0 (9)	4.0 ± 1.6 (5)	1.3 ± 0.3 (9)	2.0 ± 0.5 (9)	1.2 ± 0.3 (5)
2	DMAB → 100 ppm silymarin	6.8 ± 1.7 (4)	7.4 ± 2.4 (5)	4.2 ± 2.4 (5)	25.5 ± 9.9 (4)	27.8 ± 4.4† (5)	3.6 ± 0.5 (5)	1.3 ± 0.3 (4)	2.2 ± 0.4 (5)	1.2 ± 0.3 (5)
3	DMAB → 500 ppm silymarin	6.8 ± 2.2 (11)	6.3 ± 1.5† (3)	4.0 ± 1.2 (5)	24.7 ± 6.3 (11)	23.0 ± 3.6† (3)	3.4 ± 1.1 (5)	1.6 ± 0.3‡ (11)	3.8 ± 0.9‡ (3)	1.1 ± 0.5 (5)
4	500 ppm silymarin	—	—	3.4 ± 1.1 (5)	—	—	0.6 ± 0.5 (5)	—	—	1.2 ± 0.3 (5)
5	None	—	—	3.8 ± 0.8 (5)	—	—	0.6 ± 0.3 (5)	—	—	1.1 ± 0.2 (5)

NOTE: Numbers in parentheses are nos. of lesions or areas examined.
Abbreviation: ADC, adenocarcinoma.
*Mean ± SD.
†Significantly different from group 1 by Student's t test, $P < 0.05$.
‡Significantly different from group 1 by Student's t test, $P < 0.02$.

relevant molecular biomarker in cancer chemoprevention (43, 44). Silymarin and silibinin were reported to decrease in protein levels of cyclin D1 in prostate cancer cells (15, 17). In the present study, silymarin also suppressed cyclin D1 overexpression in prostate adenocarcinoma.

Also, treatment with silymarin inhibits the increase in cell proliferation activity caused by a radical-generating tumor promoter (20). Silymarin is known to exert an antipromoting effect on skin tumorigenesis in mice mediated by impairment of receptor and nonreceptor tyrosine kinase signaling pathway (19). Moreover, in an *in vivo* preclinical prostate cancer model, silibinin inhibits advanced human prostate carcinoma growth (30). In this study, the incidence of adenocarcinoma was decreased by the treatment with silymarin, whereas that of PIN in group 3 was slightly higher than group 1 without statistical significance. The reason for this is unknown, but it may be possible that silymarin feeding at a dose of 500 ppm inhibits progression of PIN to invasive adenocarcinoma. Feeding with silymarin lowered the PCNA labeling indices in the preneoplasms and/or carcinomas of prostate, suggesting that silymarin in diet could suppress the high-proliferative activity of cells initiated with a carcinogen. The other significant finding of this study is the apoptotic index of PIN and adenocarcinoma, which was found to be significantly greater in silymarin-fed rats. The results are in accordance with our previous studies (23, 25) and suggest that, in addition to inhibiting proliferation, apoptosis plays a significant role in inhibition of DMAB-induced prostate carcinogenesis by silymarin. Thus, in the current study, the inhibition of carcinogen-induced prostate malignancies for rats consuming silymarin in part is explained by the alteration of cell proliferating activity and/or apoptosis.

Chemoprevention of cancer might be defined as the deliberate introduction of these selected nontoxic substances into the diet for the purpose of reducing cancer development. Silymarin is clinically used to as antihepatotoxic agents and devoid of any toxicity and untoward effects in both animal and human studies (45). In the present study, the estimated daily silymarin intakes in rats given diet containing 100 and 500 ppm silymarin were ~5 and 25 mg/kg. In a direct extrapolation to a 60 kg person, these doses are equivalent to the estimated doses of clinical use as an antihepatotoxic agent (45). Recently, Singh et al. (30, 46) reported that dietary feeding of silibinin (up to 1%) to nude mice did not show any adverse effect. In the present study, administration of 500 ppm silymarin did not also show any adverse effect on diet consumption, body weight gain, prostate weight, and pathologic alteration for 40 weeks. On the other hand, silibinin is physiologically achievable in different organs including prostate as well as in plasma, and the achievable levels of total slibinin has been found in the range of 15 to 100 μmol/L in plasma by feeding with 0.05% to 1% silibinin/silymarin in rodents (30, 47, 48). The achievable levels (15-100 μmol/L) of silibinin showed inhibition of human prostate cancer cells growth in culture (16, 17, 30). These observations showed that the efficacy of silymarin at dietary dose levels without any adverse effects could have a direct practical and translational relevance to human prostate cancer patients. However, silymarin is a mixture of three structural isomers of flavonoids. Among the flavonoids, silibinin (also called silybin, silibin, or sibilinin) is suggested to be the most active constituent. Because the cancer chemopreventive and anticarcinogenic effects of silymarin seem to be due to the main constituent silibinin (16, 30, 37, 49, 50), further studies of the chemopreventive effects of silibinin itself are necessary.

In conclusion, dietary administration of silymarin significantly suppressed the development of DMAB-induced rat prostate carcinomas. Such cancer protective effect of silymarin might relate to the modulation of cell growth and apoptosis in the prostate neoplastic lesions.

References

1. Jemal A, Thomas A, Murray T, Thun M. Cancer statistics, 2002. CA Cancer J Clin 2002;52:23–47.
2. Hsing AW, Devesa SS. Trends and patterns of prostate cancer: what do they suggest? Epidemiol Rev 2001;23:3–13.
3. The Research Group for Population-Based Cancer Registration in Japan. Cancer incidence and incidence rates in Japan in 1995: estimates based on data from nine population-based cancer registries. Jpn J Clin Oncol 2000;30:318–21.
4. Shimizu H, Ross RK, Bernstein L, Yatani R, Henderson BE, Mack TM. Cancers of the prostate and breast among Japanese and White immigrants in Los Angeles county. Br J Cancer 1991;63:963–6.
5. Greco KE, Kulawiak L. Prostate cancer prevention: risk reduction through life-style, diet, and chemoprevention. Oncol Nurs Forum 1994;21:1504–11.
6. Luper S. A review of plants used in the treatment of liver disease: Part 1. Altern Med Rev 1998;3:410–21.
7. Valenzuela A, Guerra R, Videla LA. Antioxidant properties of the flavonoids silybin and (+)-cyanidanol-3: *comparison with butylated hydroxyanisole and* butylated hydroxytoluene. Planta Med 1986;52: 438–40.
8. Comoglio A, Leonarduzzi G, Carini R, et al. Studies on the antioxidant and free radical scavenging properties of IdB 1016: a new flavanolignan complex. Free Radic Res Commun 1990;11:109–15.
9. Salmi HA, Sarna S. Effect of silymarin on chemical, functional, and morphological alterations of the liver. A double-blind controlled study. Scand J Gastroenterol 1982;17:517–21.
10. Pares A, Planas R, Torres M, et al. Effects of silymarin in alcoholic patients with cirrhosis of the liver: results of a controlled, double-blind, randomized and multicenter trial. J Hepatol 1998;28:615–21.
11. Hahn G, Lehmann HD, Kurten M, Uebel H, Vogel G. On the pharmacology and toxicology of silymarin, an antihepatotoxic active principle from *Silybum marianum* (L.) Gaertn. Arzneimittelforschung 1968; 18:698–704.
12. Gershbein LL. Action of dietary trypsin, pressed coffee oil, silymarin and iron salt on 1,2-dimethylhydrazine tumorigenesis by gavage. Anticancer Res 1994;14: 1113–6.
13. Katiyar SK, Korman NJ, Mukhtar H, Agarwal R. Protective effects of silymarin against photocarcinogenesis in a mouse skin model. J Natl Cancer Inst 1997;89:556–66.
14. Mehta RG, Moon RC. Characterization of effective chemopreventive agents in mammary gland *in vitro using an initiation-promotion protocol. Anticancer* Res 1991;11:593–6.
15. Zi X, Agarwal R. Silibinin decreases prostate-specific antigen with cell growth inhibition via G_1 arrest, leading to differentiation of prostate carcinoma cells: implications for prostate cancer intervention. Proc Natl Acad Sci U S A 1999;96:7490–5.
16. Zi X, Zhang J, Agarwal R, Pollak M. Silibinin upregulates insulin-like growth factor-binding protein 3 expression and inhibits proliferation of androgen-independent prostate cancer cells. Cancer Res 2000; 60:5617–20.
17. Zi X, Grasso AW, Kung H-J, Agarwal R. A flavonoid antioxidant, silymarin, inhibits activation of erbB1 signaling and induces cyclin-dependent kinase inhibitors, G_1 arrest, and anticarcinogenic effects in human prostate carcinoma DU145 cells. Cancer Res 1998;58:1920–9.
18. Tyagi AK, Bhatia N, Condon MS, Bosland MC, Agarwal C, Agarwal R. Antiproliferative and apoptotic effects of silibinin in rat prostate cancer cells. Prostate 2002;53:211–7.
19. Lahiri-Chatterjee M, Katiyar SK, Mohan RR, Agarwal R. A flavonoid antioxidant, silymarin, affords exceptionally high protection against tumor promotion in the SENCAR mouse skin tumorigenesis model. Cancer Res 1999;59:622–32.
20. Agarwal R, Katiyar SK, Lundgren DW, Mukhtar H. Inhibitory effect of silymarin, an anti-hepatotoxic flavonoid, on 12-*O*-tetradecanoylphorbol-13-acetate-induced epidermal ornithine decarboxylase activity and mRNA in SENCAR mice. Carcinogenesis 1994; 15:1099–103.
21. Zi X, Mukhtar H, Agarwal R. Novel cancer chemopreventive effects of a flavonoid antioxidant silymarin: inhibition of m RNA expression of an endogenous tumor promoter TNFα. Biochem Biophys Res Commun 1997; 239:334–9.
22. Steele VE, Kelloff GJ, Wilkinson BP, Arnold JT. Inhibition of transformation in cultured rat tracheal epithelial cells by potential chemopreventive agents. Cancer Res 1990;50:2068–74.
23. Yanaida Y, Kohno H, Yoshida K, et al. Dietary silymarin suppresses 4-nitroquinoline 1-oxide-induced tongue carcinogenesis in male F344 rats. Carcinogenesis 2002;23:787–94.
24. Vinh PQ, Sugie S, Tanaka T, et al. Chemopreventive effects of a flavonoid antioxidant silymarin on *N*-butyl-*N*-(4-hydroxybutyl)nitrosamine-induced urinary bladder carcinogenesis in male ICR mice. Jpn J Cancer Res 2002;93:42–9.
25. Kohno H, Tanaka T, Kawabata K, et al. Silymarin, a naturally occurring polyphenolic antioxidant flavonoid, inhibits azoxymethane-induced colon carcinogenesis in male F344 rats. Int J Cancer 2002;101:461–8.
26. Mori T, Imaida K, Tamano S, et al. Beef tallow, but not perilla or corn oil, promotion of rat prostate and intestinal carcinogenesis by 3,2′-dimethyl-4-aminobiphenyl. Jpn J Cancer Res 2001;92:1026–33.
27. Bostwick DG, Brawer MK. Prostatic intra-epithelial neoplasia and early invasion in prostate cancer. Cancer 1987;59:788–94.
28. Watanabe I, Toyoda M, Okuda J, et al. Detection of apoptotic cells in human colorectal cancer by two different *in situ* methods: antibody against single-stranded DNA and terminal deoxynucleotidyl transferase-mediated dUTP-biotin nick end-labeling (TUNEL) methods. Jpn J Cancer Res 1999;90: 188–93.
29. Otori K, Sugiyama K, Fukushima S, Esumi H. Expression of the cyclin D1 gene in rat colorectal aberrant crypt foci and tumors induced by azoxymethane. Cancer Lett 1999;140:99–104.
30. Singh RP, Dhanalakshmi S, Tyagi AK, Chan DC, Agarwal C, Agarwal R. Dietary feeding of silibinin inhibits advance human prostate carcinoma growth in athymic nude mice and increases plasma insulin-like growth factor-binding protein-3 levels. Cancer Res 2002;62:3063–9.
31. Cohen SM. Cell proliferation and carcinogenesis. Drug Metab Rev 1998;30:339–57.
32. Moore MA, Tsuda H. Chronically elevated proliferation as a risk factor for neoplasia. Eur J Cancer Prev 1998;7:353–85.
33. Zi X, Feyes DK, Agarwal R. Anticarcinogenic effect of a flavonoid antioxidant, silymarin, in human breast cancer cells MDA-MB 468: Induction of G_1 arrest through an increase in Cip1/p21 concomitant with a decrease in kinase activity of cyclin-dependent kinases and associated cyclins. Clin Cancer Res 1998; 4:1055–64.
34. Sharma G, Singh RP, Chan DC, Agarwal R. Silibinin induces growth inhibition and apoptotic cell death in human lung carcinoma cells. Anticancer Res 2003; 23:2649–55.
35. Agarwal C, Singh RP, Dhanalakshmi S, et al. Silibinin upregulates the expression of cyclin-dependent kinase inhibitors and causes cell cycle arrest and apoptosis in human colon carcinoma HT-29 cells. Oncogene 2003; 22:8271–82.
36. Ahmad N, Gali H, Javed S, Agarwal R. Skin cancer chemopreventive effects of a flavonoid antioxidant silymarin are mediated via impairment of receptor tyrosine kinase signaling and perturbation in cell cycle progression. Biochem Biophys Res Commun 1998;248: 294–301.
37. Bhatia N, Zhao J, Wolf DM, Agarwal R. Inhibition of human carcinoma cell growth and DNA synthesis by silibinin, an active constituent of milk thistle: comparison with silymarin. Cancer Lett 1999;147: 77–84.
38. Sherr CJ. G_1 phase progression: cycling on cue. Cell 1994;79:551–5.
39. Motokura T, Arnold A. Cyclins and oncogenesis. Biochim Biophys Acta 1993;1155:63–78.
40. Sutter T, Doi S, Carnevale KA, Arber N, Weinstein IB. Expression of cyclins D1 and E in human colon adenocarcinomas. J Med 1997;28:285–309.
41. Sgambato A, Migaldi M, Faraglia B, et al. Cyclin D1 expression in papillary superficial bladder cancer: its association with other cell cycle-associated proteins, cell proliferation and clinical outcome. Int J Cancer 2002;97:671–8.
42. Wang QS, Papanikolaou A, Sabourin CL, Rosenberg DW. Altered expression of cyclin D1 and cyclin-dependent kinase 4 in azoxymethane-induced mouse colon tumorigenesis. Carcinogenesis 1998;19: 2001–6.
43. Weinstein IB, Begemann M, Zhou P, et al. Disorders in cell circuitry associated with multistage carcinogenesis: exploitable targets for cancer prevention and therapy. Clin Cancer Res 1997;3:2696–702.
44. Buolamwini JK. Cell cycle molecular targets in novel anticancer drug discovery. Curr Pharm Des 2000;6: 379–92.
45. Wellington K, Jarvis B. Silymarin: a review of its clinical properties in the management of hepatic disorders. BioDrugs 2001;15:465–9.
46. Singh RP, Sharma G, Dhanalakshmi S, Agarwal C, Agarwal R. Suppression of advanced human prostate tumor growth in athymic mice by silibinin feeding is associated with reduced cell proliferation, increased apoptosis, and inhibition of angiogenesis. Cancer Epidemiol Biomarkers Prev 2003;12:933–9.
47. Singh RP, Tyagi AK, Zhao J, Agarwal R. Silymarin inhibits growth and causes regression of established skin tumors in SENCAR mice via modulation of mitogen-activated protein kinases and induction of apoptosis. Carcinogenesis 2002;23:499–510.
48. Zhao J, Agarwal R. Tissue distribution of silibinin, the major active constituent of silymarin, in mice and its association with enhancement of phase II enzymes: implications in cancer chemoprevention. Carcinogenesis 1999;20:2101–8.
49. Sharma Y, Agarwal C, Singh AK, Agarwal R. Inhibitory effect of silibinin on ligand binding to erbB1 and associated mitogenic signaling, growth, and DNA synthesis in advanced human prostate carcinoma cells. Mol Carcinog 2001;30:224–36.
50. Dhanalakshmi S, Singh RP, Agarwal C, Agarwal R. Silibinin inhibits constitutive and TNFα-induced activation of NF-κB and sensitizes human prostate carcinoma DU145 cells to TNFα-induced apoptosis. Oncogene 2002;21:1759–67.

Toxicologic Pathology, 33:764–767, 2005

ISSN: 0192-6233 print / 1533-1601 online
DOI: 10.1080/01926230500416336

Lack of Urinary Bladder Carcinogenicity of Sodium L-Ascorbate in Human c-Ha-*ras* Proto-Oncogene Transgenic Rats

KEIICHIROU MORIMURA,[1] JIN SEOK KANG,[1] MIN WEI,[1] HIDEKI WANIBUCHI,[1] HIROYUKI TSUDA,[2] AND SHOJI FUKUSHIMA[1]

[1]*Department of Pathology, Osaka City University Medical School, Osaka, Japan*
[2]*Department of Molecular Toxicology, Nagoya City University Graduate School of Medical Sciences, Nagoya, Japan*

ABSTRACT

Sodium L-ascorbate (Na-AsA) is widely known to be a tumor promoter of rat bladder carcinogenesis but tests negative in standard 2-year bioassays. In the present study, bladder-cancer-susceptible transgenic rats designated Hras128 were used to further examine the tumorigenicity of Na-AsA. A total of 40 7-week-old male transgenic (Tg) and 42 littermate nontransgenic (Non-tg) rats were divided into 4 groups and given powdered MF diet with or without 5% Na-AsA for 57 weeks. Tg rats showed significantly short survival compared with Non-tg, independent of Na-AsA treatment. Tg rats treated with Na-AsA showed a slightly higher incidence of carcinoma (29.6%) as compared to those without Na-AsA treatment (15.4%), but this was without statistical significance. Moreover, the total bladder tumor incidences, including papillomas, did not differ statistically (with Na-AsA, 37.0%; without Na-AsA, 30.8%). No bladder tumor was detected in Non-tg rats. Various kinds of other lesions in various organs were noted in Tg rats treated with or without Na-AsA treatment, but no intergroup differences were evident. In conclusion, Na-AsA did not show tumorigenicity in highly bladder-cancer-susceptible transgenic Hras128 rats. These results suggest that Na-AsA is a pure promoter but not a complete carcinogen in rats.

Keywords. Urinary bladder carcinogenesis; sodium L-ascorbate; human c-Ha-*ras* proto-oncogene transgenic rats; transitional cell carcinoma; in vivo carcinogenicity bioassay; human cancer risk assessment.

INTRODUCTION

Sodium L-ascorbate (Na-AsA), like other sodium salts of saccharin (glutamate and bicarbonate), produces mild superficial urothelial cytotoxicity and regeneration (Fukushima et al., 1983, 1990; Cohen et al., 1995, 1998) when fed at high doses to rats. Na-AsA exerts a promotional effect on rat 2-stage urinary bladder carcinogenesis initiated by genotoxic bladder carcinogens such as *N*-butyl-*N*-(4-hydroxybutyl)nitrosamine (BBN) (Fukushima et al., 1983, 1990; Chen et al., 1999a, 1999b), but demonstrated no tumorigenicity for rat urinary bladder in standard 2-year carcinogenicity tests (Ellwein and Cohen, 1988, 1990; Cohen and Ellwein, 1990; Cohen et al., 1995, 1998). However, Cohen et al. (1998) did demonstrate the carcinogenic potential of Na-AsA in male rats using a 2-generation bioassay, which suggests that the period of Na-AsA treatment and/or the age of the rat at the start of the study may influence the carcinogenic potential of Na-AsA. The purpose of the present study, therefore, was to further evaluate the carcinogenicity of Na-AsA using highly bladder-cancer-susceptible animals.

Various kinds of transgenic and knockout mice are now established as providing good animal models for analysis of gene functions, especially those relevant to carcinogenesis. Some of these animals exhibit high susceptibility to chemical carcinogens in a tissue-specific manner, and now they are receiving much attention with regard to potential application in carcinogenicity tests for risk assessment.

Asamoto et al. (2000) have established a transgenic rat carrying 3 copies of the human c-Ha-*ras* proto-oncogene with its own promoter region, designated Hras128, which is highly susceptible to induction of tumors in mammary tissue by N-methyl-N-nitrosourea (MNU) and 7,12-dimrthylbenz[*a*]anthracene (DBMA) (Asamoto et al., 2000; Tsuda et al., 2001; Fukamachi et al., 2004), and also in the esophagus by N-nitrosomethylbenzylamine (Asamoto et al., 2002) and in the skin by DMBA treatment with or without 12-*O*-tetradecanoylphorbol 13-acetate (TPA) promotion (Park et al., 2004). Moreover, this strain shows remarkable susceptibility to bladder carcinogenesis induced by BBN (Ota et al., 2000).

In the present study, to further assess the tumorigenicity of Na-AsA in the rat urinary bladder, we used this species of cancer-susceptible transgenic rat in a long-term carcinogenicity test.

MATERIALS AND METHODS

Animals

The Hras128 rat line (Asamoto et al., 2000) was generated by injecting copies of the human c-Ha-*ras* proto-oncogene into pronuclei of fertilized rat oocytes from Sprague–Dawley rats obtained from Clea Japan, Inc. (Tokyo, Japan). Subsequent matings were carried out between Tg and Non-tg Sprague–Dawley rats to maintain rat heterozygotes for the transgene (Clea Japan Inc., Tokyo). All the rats subjected to this study were confirmed for the genotype at Clea Japan Inc. (Tokyo, Japan).

Address correspondence to: Shoji Fukushima, Prof. and Chairman, Department of Pathology, Osaka City University Medical School, 1-4-3, Asahi-machi, Abeno-ku, Osaka 545-8585, Japan; e-mail: fukuchan@med.osaka-cu.ac.jp

Sodium ascorbate, Na-AsA; *N*-butyl-*N*-(4-hydroxybutyl)nitrosamine, BBN; transitional cell carcinoma, TCC.

Experimental Protocol

A total of 40 7-week-old male Tg rats were divided into 2 groups. Twenty-seven (group 1) and 13 (group 2) rats were given a powdered MF diet (Oriental Yeast Co., Ltd., Tokyo) with or without 5% Na-AsA (Wako Pure Chemical Industries, Tokyo Japan), respectively. Similarly, a total of 42 7-week-old male Non-tg rats were divided into 2 groups, and 30 (group 3) and 12 (group 4) animals were given a diet with or without 5% Na-AsA, respectively.

Animals were housed in groups of 2 to 3 in plastic cages with hard wood chips for bedding in an animal room with a 12-hour light, 12-hour dark cycle at a temperature of 22 ± 2°C and a humidity of 55 ± 5%. Body weights were measured weekly, and food consumption and water intake were calculated biweekly during the course of the experiment. Animals were carefully monitored until being sacrificed at final week 57 of the experimental period. Those becoming moribund during the course of the study, or when tumors appeared externally, were sacificed under ether anesthesia for autopsy and macroscopic and microscopic examinations.

All the animal experimental procedures used were approved by the Institutional Animal Care and Use Committee of Osaka City University Medical School.

Histological Examinations

All the animals were sacrificed under ether anesthesia at 57 weeks from the beginning of the experiment. Major organs including skin/subcutaneous tissue, mammary gland, forestomach, glandular stomach, small and large intestine, liver, pancreas, lung, kidney, testis, prostate, thymus, spleen, and urinary bladder were macroscopically examined. Any tumors apparent in those various organs were collected. Tissues were fixed in 10% phosphate-buffered formalin, embedded in paraffin, and sectioned for routine hematoxylin and eosin staining for histopathological analysis. Urinary bladder lesions were classified based on the WHO International Classification of Rodent Tumors (Kunze and Chowaniec, 1990).

Statistical Analysis

Surviving curves were created using the Kaplan–Meier method, and the statistical significance of differences was calculated by the log-rank test. Variations in incidences of tumors between the different treatments or animal types were evaluated with the nonparametric Fisher's exact probability test or the χ^2 test. All the calculations for statistical analysis were performed using the Statview SE+ Graphics, version 5.0 (Abacus Concepts, Berkeley, CA).

RESULTS

Survival Rates

Tg rats harbored various kinds of spontaneous tumors in various organs when the experiment was terminated after 57 weeks. Survival curves for all groups are shown in Figure 1. As a whole, Tg rats showed a short lifetime, regardless of 5% Na-AsA treatment (groups 1 and 2), compared with their littermate Non-tg rats (groups 3 and 4), but no significant differences were noted between group 1 and group 2 ($p = 0.4001$). About half of group 1 had died or been sacrificed due to the weight loss and/or tumor latency, and group 1's survival

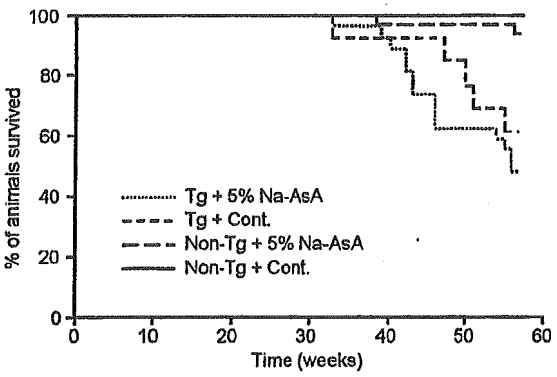

FIGURE 1.—Survival curves of all groups. The experiment was termed at 57 weeks with final sacrificing of all animals.

curve was significantly different from that of group 3 ($p < 0.0001$). The survival curves for groups 3 and 4 were similar. A significant difference was also evident between groups 2 and 4 ($p < 0.05$). No animal died throughout the study in group 4, and 2 animals in group 3 died from pneumonia and fibrosarcoma of subcutaneous tissue with lung metastasis, respectively.

Tumor Incidences

Table 1 summarizes data for incidences of bladder tumors. All the lesions were transitional cell papillomas or carcinomas (Figure. 2A, B), and no bladder tumors occurred in either groups 3 or 4. No difference in the combined overall incidence of transitional cell carcinomas and papillomas was detected between groups 1 (37.0%) and 2 (30.8%). There was a tendency for Tg rats treated with Na-AsA to show a higher incidence of carcinoma (29.6%), compared to those without Na-AsA (15.4%), but no statistical difference was noted. Simple hyperplasia was detected in all the rats treated with Na-AsA, regardless of genotype.

Incidences of tumor-bearing rats in groups 1, 2, 3, and 4 were 70.3, 69.2, 20.0, and 25.0%, respectively (Table 2). The Tg rats showed significantly high incidences of tumors compared with Non-tg rats, both with and without Na-AsA treatment. However, there was no statistical difference between groups 1 and 2. A summary of tumors generated in organs other than the bladder is given in Table 3. Independent of the Na-AsA treatment, transgenic rats exhibited various kinds of malignant tumors in various organs, without significant differences between groups 1 and 2.

DISCUSSION

In 1998, Cohen et al. (1998) examined the tumorigenicity of Na-AsA in male rats using a 2-generation bioassay

TABLE 1.—Tumor incidences in urinary bladder.

Groups	1	2	3	4
No. of rats	27	13	30	12
Papilloma	2 (7.4)[a]	2 (15.4)	0 (0)	0 (0)
TCC	8 (29.6)	2 (15.4)	0 (0)	0 (0)
Total	10 (37.0)	4 (30.8)	0 (0)	0 (0)

[a] % in parenthesis.
TCC, Transitional cell carcinoma.

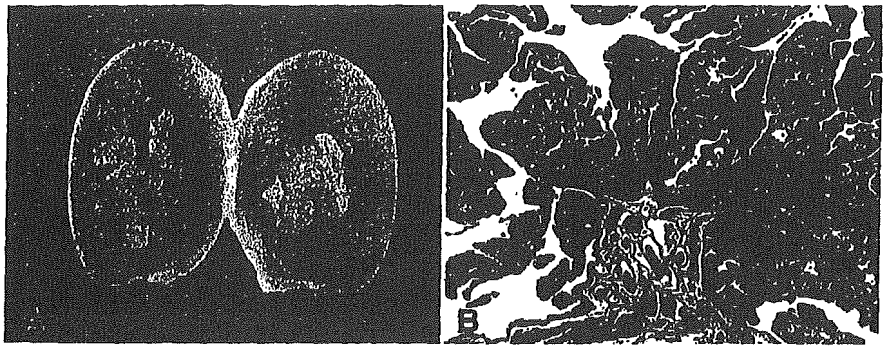

FIGURE 2.—Macroscopic (A) and microscopic (B) appearances of bladder transitional cell carcinoma in Hras128 rat.

that involved feeding to the male and female parental rats for 4 weeks before mating, feeding the dams during gestation and lactation, and then feeding the weaned male F_1 generation rats for the remainder of their lifetime. In that experiment, high-dose (5.0 and 7.0%) treatment of Na-AsA demonstrated an increase in urinary bladder urothelial papillary, nodular hyperplasia, and even papillomas and carcinomas with dose dependence. This implies the possibility of bladder cancer production on the part of this chemical, but no positive cancer induction has been observed thus far in standard, 1-generation-carcinogenicity tests using rodent models.

In the present study, a reexamination of the rat bladder carcinogenesis of the Na-AsA of Hras128 rat, a highly susceptible strain, provided no evidence of cancer induction. The nonsignificant tendency for an increase in the number of malignant tumors in Tg rats suggests the possibility of a weak promotion effect after spontaneous initiation.

Transgenic mice carrying human c-Ha-ras protooncogenes (rasH2) are highly susceptible to various carcinogens and have been demonstrated to be more predictive of human response than the classical cancer test methods (Mitsumori, 2003). This animal model is now regarded as a useful tool for evaluating chemical carcinogenicity, in accordance with the recommendation of the International Conference on Harmonization of Technical Requirements of Pharmaceuticals for Human Use (ICH). However, Na-AsA is not known to exert an enhancing influence on mice bladder carcinogenesis after BBN treatment (Tamano et al., 1993). Therefore, we employed a rat model to evaluate the carcinogenicity of Na-AsA.

In rodent urinary bladder carcinomas, those induced by BBN with and/or without Na-AsA in rats are mostly of the superficial type, while the invasive type is more frequent in mice. Moreover, almost all of the bladder cancers in rats are TCCs, whereas in mice most are squamous cell carcinomas. In the human bladder, TCCs are a major histological type, and this is classified as a "superficial type." They are associated with frequent recurrence and invasion to the muscle layer, resulting in the poor prognosis. However, the reasons for such recurrence and invasive characteristics have not yet been elucidated in detail. We used a rat transgenic animal model representing the superficial type to reexamine the carcinogenic potential of Na-AsA, to match the histological type of human bladder carcinomas.

Ota et al. (2000) examined the susceptibility of bladder carcinogenesis in the same Tg rats using the potent genotoxic carcinogen, BBN, and revealed a high incidence of bladder carcinomas. Also, the Hras128 rat was found to exhibit greater tumor progression as compared to Non-tg counterparts. Mutations of both the exogenous and endogenous c-Ha-*ras* gene are rare, which may indicate that enhanced tumor development was not due primarily to mutations occurring in the transgene. The authors concluded that the overexpression of total c-Ha-ras protein, due to the expression of integrated genes, plays a major role in rat bladder carcinogenesis. Taking these findings into account, the molecular target of Na-AsA in enhancing bladder cancer production may differ from the c-Ha-*ras* overexpression pathway.

TABLE 2.—Effect of 5% Na-AsA in Hras128 rats.

Groups	Strain and treatment	No. of rats	No. of tumor-bearing rats
1	Tg + 5% Na-AsA	27	19 (70.3)[a,b]
2	Tg + Cont.	13	9 (69.2)[c]
3	Non-Tg + 5% Na-AsA	30	6 (20.0)
4	Non-Tg + Cont.	12	3 (25.0)

[a] % in parenthesis.
[b] Statistically significant with its Non-tg + 5% Na-AsA ($p < 0.0001$).
[c] Statistically significant with its Non-tg + Cont. ($p < 0.01$).
Tg, Hras128; Na-AsA, Sodium L-ascorbate in diet; Cont., Control diet.

TABLE 3.—Summary of tumors in various organs.

Groups	1	2	3	4
No. of rats	27	13	30	12
Mammary				
Fibroadenoma	0 (0)[a]	0 (0)	0 (0)	1 (8.3)
Adenocarcinoma	3 (11.1)	1 (7.7)	1 (3.3)	0 (0)
Liver				
Adenoma	1 (3.7)	0 (0)	0 (0)	0 (0)
Cholangiocarcinoma	1 (3.7)	0 (0)	0 (0)	0 (0)
Kidney				
Adenoma	0 (0)	1 (7.7)	0 (0)	0 (0)
Thymus				
Lymphoma	1 (3.7)	0 (0)	0 (0)	0 (0)
Skin and subcutis				
Sebaceous adenoma	1 (3.7)	0 (0)	0 (0)	2 (16.7)
Keratoacanthoma	1 (3.7)	0 (0)	2 (6.7)	0 (0)
Squamous cell papilloma	1 (3.7)	0 (0)	0 (0)	0 (0)
Squamous cell carcinoma	1 (3.7)	3 (23.1)	1 (3.3)	0 (0)
Basal cell carcinoma	1 (3.7)	0 (0)	1 (3.3)	0 (0)
Fibrosarcoma	3 (11.1)	2 (15.4)	1 (3.3)	0 (0)
Malignant fibrous histiocytoma	1 (3.7)	0 (0)	0 (0)	0 (0)

[a] % in parenthesis.

In conclusion, the rat bladder promoter Na-AsA did not show tumorigenicity, even when administered to highly bladder-cancer-susceptible Hras128 rats. However, the tendency for an increase of malignancy in Tg rats' bladder tumors suggests that Na-AsA may have promotional effects. Taking the previous reports into account, these results suggest that Na-AsA is a pure promoter but not a complete carcinogen in rats.

ACKNOWLEDGMENT

We wish to thank M. Imanaka and K. Touma for their expert technical assistance. We also are indebted to M. Dokoh, Y. Onishi, and Y. Shimada for assistance in preparing the manuscript. This work was supported by Grants-in-Aid for Cancer Research from the Ministry of Health, Labor and Welfare in Japan.

REFERENCES

Asamoto, M., Ochiya, T., Toriyama-Baba, H., Ota, T., Sekiya, T., Terada, M., and Tsuda, H. (2000). Transgenic rats carrying human c-Ha-ras proto-oncogenes are highly susceptible to *n*-methyl-*n*-nitrosourea mammary carcinogenesis. *Carcinogenesis* **21**, 243–9.

Asamoto, M., Toriyama-Baba, H., Ohnishi, T., Naito, A., Ota, T., Ando, A., Ochiya, T., and Tsuda, H. (2002). Transgenic rats carrying human c-Ha-ras proto-oncogene are highly susceptible to *n*-nitrosomethylbenzylamine induction of esophageal tumorigenesis. *Jpn J Cancer Res* **93**, 744–51.

Chen, T. X., Wanibuchi, H., Murai, T., Kitano, M., Yamamoto, S., and Fukushima, S. (1999a). Promotion by sodium L-ascorbate in rat two-stage urinary bladder carcinogenesis is dependent on the interval of administration. *Jpn J Cancer Res* **90**, 16–22.

Chen, T. X., Wanibuchi, H., Wei, M., Morimura, K., Yamamoto, S., Hayashi, S., and Fukushima, S. (1999b). Concentration dependent promoting effects of sodium L-ascorbate with the same total dose in a rat two-stage urinary bladder carcinogenesis. *Cancer Lett* **146**, 67–71.

Cohen, S. M., Anderson, T. A., de Oliveira, L. M., and Arnold, L. L. (1998). Tumorigenicity of sodium ascorbate in male rats. *Cancer Res* **58**, 2557–61.

Cohen, S. M., and Ellwein, L. B. (1990). Cell proliferation in carcinogenesis. *Science* **249**, 1007–11.

Cohen, S. M., Garland, E. M., Cano, M., St John, M. K., Khachab, M., Wehner, J. M., and Arnold, L. L. (1995). Effects of sodium ascorbate, sodium saccharin and ammonium chloride on the male rat urinary bladder. *Carcinogenesis* **16**, 2743–50.

Ellwein, L. B., and Cohen, S. M. (1988). A cellular dynamics model of experimental bladder cancer: analysis of the effect of sodium saccharin in the rat. *Risk Anal* **8**, 215–21.

Ellwein, L. B., and Cohen, S. M. (1990). The health risks of saccharin revisited. *Crit Rev Toxicol* **20**, 311–26.

Fukamachi, K., Han, B. S., Kim, C. K., Takasuka, N., Matsuoka, Y., Matsuda, E., Yamasaki, T., and Tsuda, H. (2004). Possible enhancing effects of atrazine and nonylphenol on 7,12-dimethylbenz[a]anthracene-induced mammary tumor development in human c-Ha-ras proto-oncogene transgenic rats. *Cancer Sci* **95**, 404–10.

Fukushima, S., Imaida, K., Sakata, T., Okamura, T., Shibata, M., and Ito, N. (1983). Promoting effects of sodium L-ascorbate on two-stage urinary bladder carcinogenesis in rats. *Cancer Res* **43**, 4454–7.

Fukushima, S., Uwagawa, S., Shirai, T., Hasegawa, R., and Ogawa, K. (1990). Synergism by sodium L-ascorbate but inhibition by L-ascorbic acid for sodium saccharin promotion of rat two-stage bladder carcinogenesis. *Cancer Res* **50**, 4195–8.

Kunze, E., and Chowaniec, J. (1990). *Pathology of Tumours in Laboratory Animals, Volume 1. Tumours of the Rat—Tumors of the urinary bladder*, Lyon, France.

Mitsumori, K. (2003). Possible mechanism on enhanced carcinogenesis of genotoxic carcinogens and unsolved mechanisms on lesser carcinogenic susceptibility to some carcinogens in rasH2 mice. *J Toxicol Sci* **28**, 371–83.

Ota, T., Asamoto, M., Toriyama-Baba, H., Yamamoto, F., Matsuoka, Y., Ochiya, T., Sekiya, T., Terada, M., Akaza, H., and Tsuda, H. (2000). Transgenic rats carrying copies of the human c-Ha-ras proto-oncogene exhibit enhanced susceptibility to *n*-butyl-*n*-(4-hydroxybutyl)nitrosamine bladder carcinogenesis. *Carcinogenesis* **21**, 1391–6.

Park, C. B., Fukamachi, K., Takasuka, N., Han, B. S., Kim, C. K., Hamaguchi, T., Fujita, K., Ueda, S., and Tsuda, H. (2004). Rapid induction of skin and mammary tumors in human c-Ha-ras proto-oncogene transgenic rats by treatment with 7,12-dimethylbenz[a]anthracene followed by 12-O-tetradecanoylphorbol 13-acetate. *Cancer Sci* **95**, 205–10.

Tamano, S., Asakawa, E., Boomyaphiphat, P., Masui, T., and Fukushima, S. (1993). Lack of promotion of *n*-butyl-*n*-(4-hydroxybutyl)nitrosamine-initiated urinary bladder carcinogenesis in mice by rat cancer promoters. *Teratog Carcinog Mutagen* **13**, 89–96.

Tsuda, H., Asamoto, M., Ochiya, T., Toriyama-Baba, H., Naito, A., Ota, T., Sekiya, T., and Terada, M. (2001). High susceptibility of transgenic rats carrying the human c-Ha-ras proto-oncogene to chemically-induced mammary carcinogenesis. *Mutat Res* **477**, 173–82.

Available online at www.sciencedirect.com
SCIENCE DIRECT
ELSEVIER
European Journal of Pharmacology 508 (2005) 23–30
ejp
www.elsevier.com/locate/ejphar

Characterization of voltage-dependent gating of $P2X_2$ receptor/channel

Ken Nakazawa[a,*], Yasuo Ohno[b]

[a]*Cellular and Molecular Pharmacology Section, Division of Pharmacology, National Institute of Health Sciences, 1-18-1 Kamiyoga, Setagaya, Tokyo 158-8501, Japan*
[b]*Division of Pharmacology, National Institute of Health Sciences, 1-18-1 Kamiyoga, Setagaya, Tokyo 158-8501, Japan*

Received 9 September 2004; received in revised form 29 November 2004; accepted 6 December 2004
Available online 4 January 2005

Abstract

The role of a voltage-dependent gate of recombinant $P2X_2$ receptor/channel was investigated in *Xenopus* oocytes. When a voltage step to −110 mV was applied from a holding potential of −50 mV, a gradual increase was observed in current evoked by 30 μM ATP. Contribution of this voltage-dependent component to total ATP-evoked current was greater when the current was evoked by lower concentrations of ATP. The voltage-dependent gate closed upon depolarization, and half the gates were closed at −80 mV. On the other hand, a potential at which half the gates opened was about −30 mV or more positive, which was determined using a series of hyperpolarization steps. The results of the present study suggest that the voltage-dependent gate behavior of $P2X_2$ receptor is not due to simple activation and deactivation of a single gate, but rather due to transition from a low to a high ATP affinity state.

Keywords: P2X receptor; Voltage dependence; Gate; Kinetics; Ligand affinity

1. Introduction

Extracellular ATP is considered a neurotransmitter, and its fast neurotransmission is mediated through ion channel-forming P2X receptors (see reviews, Ralevic and Burnstock, 1998; Khakh, 2001; North, 2002). To date, at least seven subclasses of P2X receptor ($P2X_{1-7}$) have been cloned, which form homo- or heteromeric receptors that act as functional ion channels (North and Surprenant, 2000). Each subclass consists of two transmembrane domains (TM1 and TM2) and one long extracellular domain (E1) between them. Both TM1 (Jiang et al., 2001; Haines et al., 2001) and TM2 (Rassendren et al., 1997; Egan et al., 1998; Migita et al., 2001) contribute to formation of the channel pore. P2X receptor/channels are permeable to cations, but demonstrate poor cation selectivity. The channels are gated by ATP molecules, and the narrowest part of the channel pore opens when activated (Rassendren et al., 1997). The ATP-binding site for gating is partly attributable to basic amino acid residues near the outer mouth of the channel pore formed by TM1 and TM2 (Ennion et al., 2000; Jiang et al., 2000), and the possibility that aromatic residues in E1 contribute to the binding site has also been suggested (Nakazawa et al., 2002; Roberts and Evans, 2004).

In addition to ATP, other factors are known to modulate channel activity. Zn^{2+} and acidic conditions facilitate ATP-mediated gating by increasing ATP sensitivity of $P2X_2$ receptor (Clyne et al., 2002). Neurotransmitters, including dopamine, and related compounds also facilitate ATP-mediated gating (Nakazawa et al., 1997a). Membrane potential may also play a role. It has been reported that ionic current activated by ATP is enhanced by hyperpolarization in pheochromocytoma PC12 cells (Nakazawa et al., 1997b). We observed similar voltage-dependent gating of recombinant $P2X_2$ receptor/channel, which was originally cloned from PC12 cells (Brake et al., 1994), and qualitatively analyzed its properties in the present study.

2. Methods

Recordings of ionic current through recombinant $P2X_2$ receptor/channels were performed according to our previous

* Corresponding author. Tel.: +81 3 3700 9704; fax: +81 3 3707 6950.
E-mail address: nakazawa@nihs.go.jp (K. Nakazawa).

0014-2999/$ - see front matter © 2004 Elsevier B.V. All rights reserved.
doi:10.1016/j.ejphar.2004.12.005

report (Nakazawa and Ohno, 1997). Briefly, the cloned rat $P2X_2$ receptor (Brake et al., 1994) was expressed in *Xenopus* oocytes by injecting in vitro transcribed cRNA. After 4 days of incubation at 18 °C, the membrane current of the oocytes was recorded. Oocytes were bathed in ND96 solution containing (in mM) NaCl 96, KCl 2, $CaCl_2$ 1.8, $MgCl_2$ 1, HEPES 5 (pH 7.5 with NaOH). In some experiments, oocytes were bathed in solution containing 10.8 mM $BaCl_2$ instead of 1.8 mM $CaCl_2$. When achieving a low extracellular chloride concentration, 96 mM Na-acetate was added instead of 96 mM NaCl. ATP (adenosine 5′-triphosphate disodium salt; Sigma, St. Louis, MO, U.S.A.) was applied by superfusion for approximately 10 s at regular 2-min intervals. Membrane current was recorded using the standard two-electrode voltage-clamp techniques, and electrical signals were stored on a data recorder (PC204Ax; SONY, Tokyo, Japan) for off-line analysis. Curve fittings to data were made using Microsoft' Excel X.

3. Results

3.1. Voltage-dependent component of ATP-evoked current

Fig. 1A compares membrane currents in the absence and presence of 30 μM ATP in a $P2X_2$ receptor-expressing oocyte. The oocyte was held at −50 mV and stepped to −110 mV for 200 ms. In the presence of ATP, inward current at −110 mV did not instantaneously reach steady-state, but gradually increased: a biphasic increase in current was observed with a voltage-independent component ("a" in Fig. 1A) and a voltage-dependent component ("b" in Fig. 1A). When the voltage was returned to −50 mV, a gradually declining inward "tail" current was observed ("c" in Fig. 1A). The voltage-dependent component of the inward current at −110 mV was observed to follow first-order kinetics with a time constant of 40 ms (Fig. 1B).

Fig. 2A demonstrates an increased magnitude of the voltage-dependent component when activated from a less negative holding potential. The voltage-dependent component was larger when the step to −110 mV was applied from −10 mV ("a" in Fig. 2A) than when it was applied from −70 mV ("b" in Fig. 2A). This dependence of the voltage-dependent component on holding potentials is illustrated in Fig. 2B. It is worth noting that Ca^{2+}-activated currents exist in *Xenopus* oocytes (Weber, 1999; Zhang and Hamill, 2000). Since P2X receptor/channels are Ca^{2+}-permeable (Khakh, 2001), a secondarily activated Ca^{2+}-induced current might contribute to the observed voltage-dependent changes. This does not, however, appear to be the case since a similar dependence on holding potentials was observed when extracellular Ca^{2+} was replaced with 10.8 mM Ba^{2+}. Time constants for the activation of the voltage-dependent component were obtained as shown in Fig. 1B, and the mean values were plotted against holding potentials

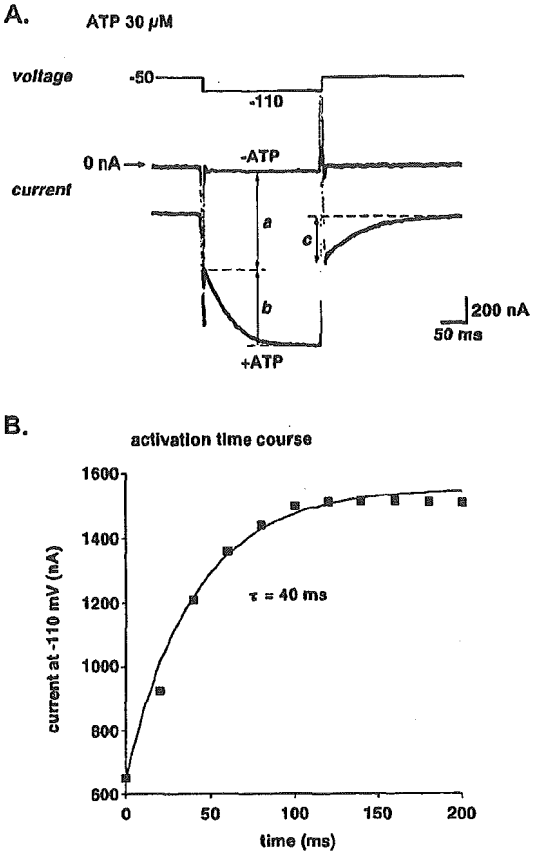

Fig. 1. (A) Current traces of an oocyte stepped to −110 mV from a holding potential of −50 mV in the absence (−ATP) or presence (+ATP) of 30 μM ATP. The current evoked by ATP is represented by the difference between the two traces. Upon hyperpolarization, a gradual increase in current was observed in the presence of ATP, suggesting activation of a voltage-dependent gate (denoted by "b"). The current denoted by "c" represents a gradually declining "tail current" that was observed when the voltage was returned to −50 mV. (B) Time course of activation of the voltage-dependent component. Current amplitude of the voltage-dependent component represented by "b" in panel A was plotted against time after the onset of hyperpolarization at −110 mV. The voltage-dependent component could be made to fit a curve with a time constant of 40 ms.

(Fig. 2C). While the current amplitude demonstrated voltage dependence (Fig. 2B), voltage did not have an effect on time course of the activation.

3.2. Effect of ATP concentrations

Fig. 3A shows the voltage-dependent component of the current activated by 10 μM or 300 μM of ATP in a single oocyte. The relative size of the voltage-dependent component involved in total ATP-evoked current became smaller when the current was evoked by greater concentrations of ATP (Fig. 3A and B). A similar dependence on ATP concentration was observed for the current evoked in the presence of 10.8 mM Ba^{2+} instead of 1.8 mM Ca^{2+} (Fig. 3B). Dependence on ATP concentrations was also found for activation time constants for the voltage-

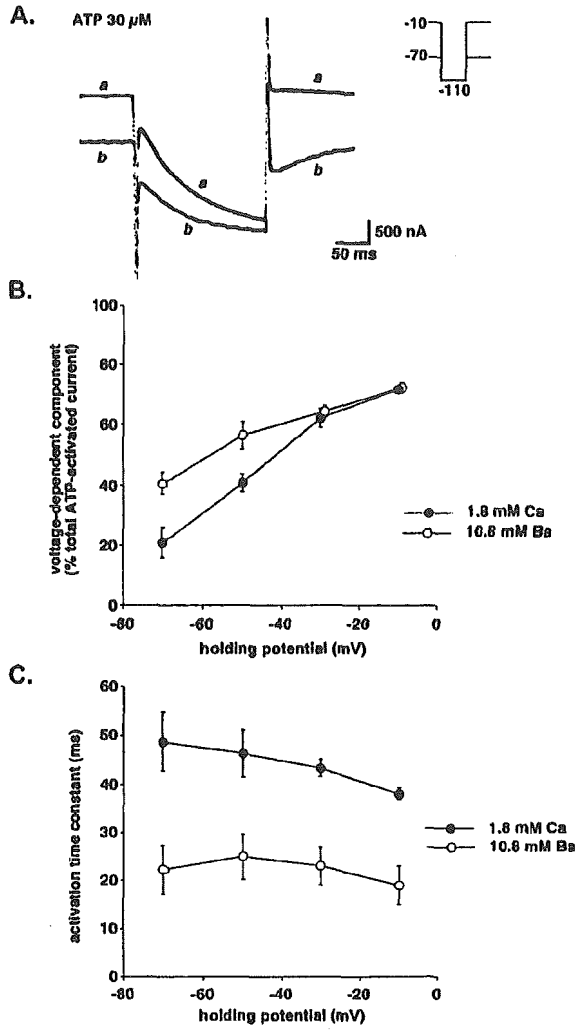

Fig. 2. Effect of holding potential on current. Current was evoked by 30 μM ATP. (A) Voltage-dependent current at −110 mV when stepped from a holding potential of −10 mV ("a") or −70 mV ("b"). (B) Effect of holding potential on voltage-dependent current. The amplitude of the voltage-dependent current was measured as described in Fig. 1A. Mean values obtained from 4 oocytes in a standard extracellular solution containing 1.8 mM Ca^{2+} (●) and an extracellular solution containing 10.8 mM Ba^{2+} (instead of Ca^{2+}; ○) were plotted. Bars represent the S.E.M. (C) Time course of activation of the voltage-dependent component. Time constants were determined as shown in Fig. 1B, and mean values obtained from 4 oocytes were plotted against holding potentials. Bars represent the S.E.M.

dependent component; the time constants were larger for 10 μM ATP than 30 μM ATP (Fig. 3C).

3.3. Activation and deactivation kinetics

Cl^- currents are observed in *Xenopus* oocytes (Weber, 1999; Zhang and Hamill, 2000). In the following experiments, current measurements were made using an extracellular solution containing 96 mM Na-aspartate instead of NaCl in order to facilitate the analysis of the voltage-dependent component of ATP-evoked current by reducing Cl^- currents. In doing so, there was an obvious reduction in outward current upon depolarization, resulting in better voltage-clamp conditions. Using this extracellular solution, the EC_{50} value for ATP-activated current measured at −50 mV was about 40 μM, which was lower than the value obtained with the standard extracellular solution containing 96 mM NaCl (about 100 μM; Nakazawa and Ohno, 2004). Fig. 4 illustrates

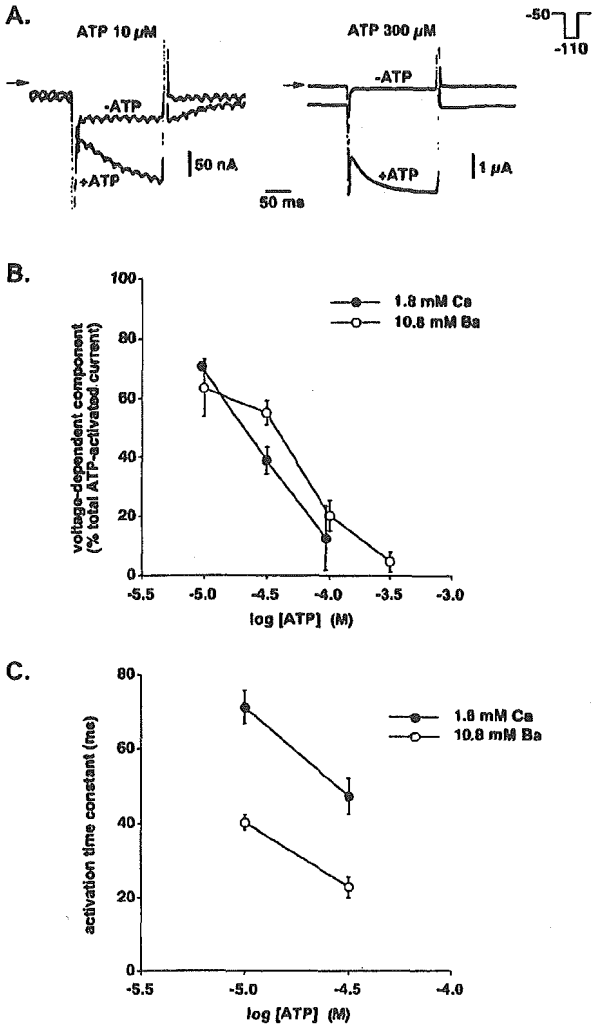

Fig. 3. Effect of ATP concentration. The voltage-dependent current was activated by hyperpolarization (−110 mV) from a holding potential of −50 mV. (A) Voltage-dependent current activated by 10 μM or 30 μM ATP. Current traces in the absence (−ATP) or presence (+ATP) of ATP are superimposed in each panel. (B) Contribution of the voltage-dependent current to total ATP-evoked current using different ATP concentrations. Mean values obtained from 4 oocytes in a standard extracellular solution containing 1.8 mM Ca^{2+} (●) and an extracellular solution containing 10.8 mM Ba^{2+} (instead of Ca^{2+}; ○) were plotted. Bars represent the S.E.M. (C) Time course of activation of the voltage-dependent components. Time constants were determined as shown in Fig. 1B, and mean values obtained from 4 oocytes were plotted against holding potentials. Bars represent the S.E.M.

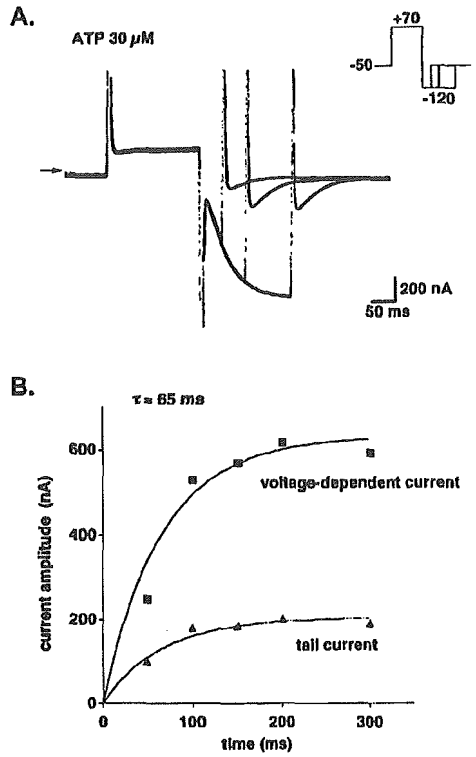

Fig. 4. Activation and tail current. (A) Gradual increase in magnitude of the tail current with increasing voltage-dependent current. Current traces obtained upon exposure to hyperpolarizing pulses (−120 mV) of different durations are superimposed. (B) Time course of activation of the voltage-dependent (■) and tail (▲) currents. Current amplitude was plotted against duration of hyperpolarization (also shown in panel A). The results of both time course activation experiments fit curves with a single time constant of 65 ms.

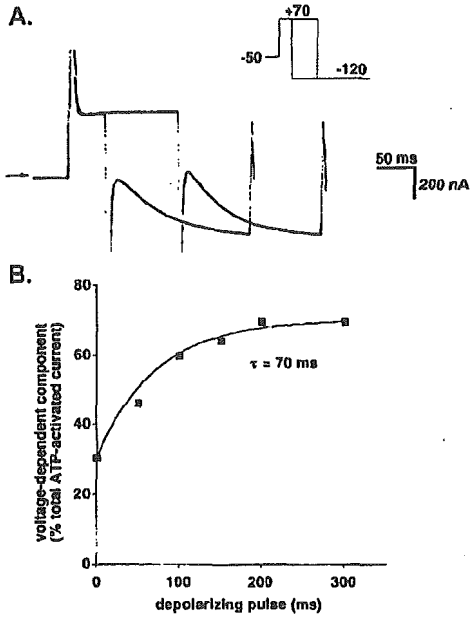

Fig. 5. Deactivation of the voltage-dependent component. (A) Current traces obtained using depolarizing pulses (+70 mV) of two different durations. The amplitude of the voltage-dependent component increased when the duration was prolonged. (B) Time course of deactivation of the voltage-dependent component. Current amplitude was plotted against duration of the depolarizing pulses (also shown in panel A).

the relation between activation kinetics of the voltage-dependent component and time course of tail current. As shown in Fig. 4A, oocytes were stepped to 70 mV and then to −120 mV to induce the voltage-dependent component. When hyperpolarization at −120 mV was terminated after various periods, a gradual increase in amplitude of the tail current was observed with increased duration of hyperpolarization at −120 mV. Time courses of both the voltage-dependent component and tail current could be fitted with curves with a single time constant (65 ms in this case; Fig. 4B). Similar fitting with single time constants were made for 4 oocytes tested, and the mean time constant±S.E.M. was 66.3±2.4 ms.

With increased duration of the +70 mV depolarizing pulse, increased amplitude of the voltage-dependent component was observed at −120 mV (Fig. 5A). This may reflect "deactivation" of the voltage-dependent component (Scheme 1):, where A is ATP, and R and R* are closed and open states, respectively, of the voltage-dependent component of $P2X_2$ receptor/channel. The deactivation time course could be fitted with a time constant of 70 ms in this case (Fig. 5B; mean±S.E.M., 71.3±1.3 ms; n=4).

3.4. Voltage dependence of activation and deactivation

As shown in Fig. 1, contribution of the voltage-dependent component to total ATP-evoked current was influenced by the holding potential prior to hyperpolarization. This was further examined by testing a number of prepulses at various potentials prior to hyperpolarization (Fig. 6A). As the prepulse became more depolarized, a greater contribution of the voltage-dependent component to total ATP-evoked current was observed, and this contribution became maximal near 0 mV (Fig. 6B). Thus, the voltage-dependent gate must be completely closed at potentials equal to or more positive than 0 mV. The data were fitted with a curve in accordance with the following model of "deactivation":

$$d_\infty = 1/\{1 + \exp[(E_{1/2} - E_m)/k]\}, \quad (1)$$

where d_∞ represents the relative proportion of closed gates at steady state, $E_{1/2}$ is the voltage at which the half-maximal closing occurs, E_m is the membrane potential, and

$$A{\cdot}R \underset{\text{(deactivation)}}{\overset{\text{(activation)}}{\rightleftharpoons}} A{\cdot}R^*$$

Scheme 1.

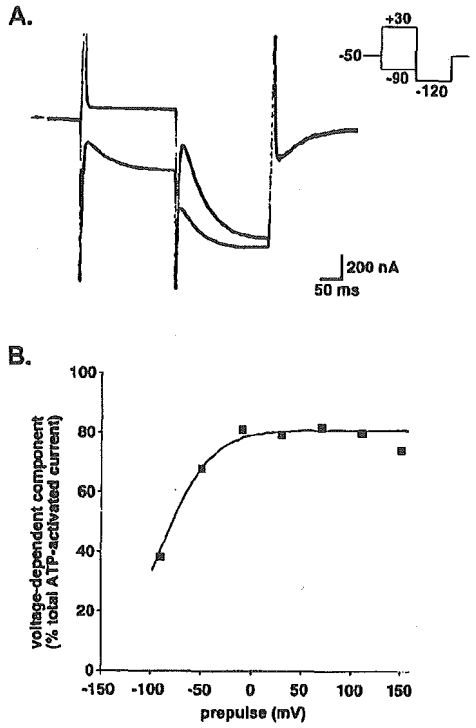

Fig. 6. Prepulse experiment. An ATP concentration of 30 μM was used. (A) Current traces obtained using prepulses of +30 mV ("a") or −90 mV ("b") prior to hyperpolarization at −120 mV. (B) Effect of prepulses. The relative contribution of the voltage-dependent current to total ATP-evoked current at −120 mV was plotted against each prepulse voltage. Some of this data is also shown in panel A.

k is a slope factor reflecting an energy barrier (Hodgkin and Huxley, 1952; Hille, 1992a). As shown in Fig. 6B, potential at which half the gates closed was estimated to be −90 mV in this case (mean±S.E.M., −78.8±5.2 mV; n=4).

The voltage dependence of activation was also examined. As shown in Fig. 7A, the channels responsible for the voltage-dependent component was sufficiently "deactivated" by applying a prepulse of +100 mV, and they were then activated at various hyperpolarization potentials. Contribution of the voltage-dependent component to total ATP-evoked current decreased as the hyperpolarization became more negative up to −45 mV in the case shown in Fig. 7B. Potentials exceeding −45 mV could not be examined since the resultant ATP-evoked current was not large enough to analyze. The data were fitted in accordance with the following model of "activation":

$$a_\infty = 1/\{1+\exp[(E_{1/2}-E_m)/k]\}, \quad (2)$$

where a_∞ represents the degree of gate opening at steady state. The other parameters are the same as those described above. The data obtained using Eq. (2) (Fig. 7B) could be fitted with a curve indicating that half of the gates were open at a potential of −30 mV.

The above data suggest that activation of the voltage-dependent gate occurs at more positive potentials than gate deactivation. To further investigate this, the fraction of the gates that escaped deactivation ($1-d_\infty$) was calculated from the data obtained during deactivation experiments. The deactivation data was then plotted alongside data obtained from activation experiments (Fig. 7C). These data suggest that the activation potential is 50 mV more positive than the deactivation potential.

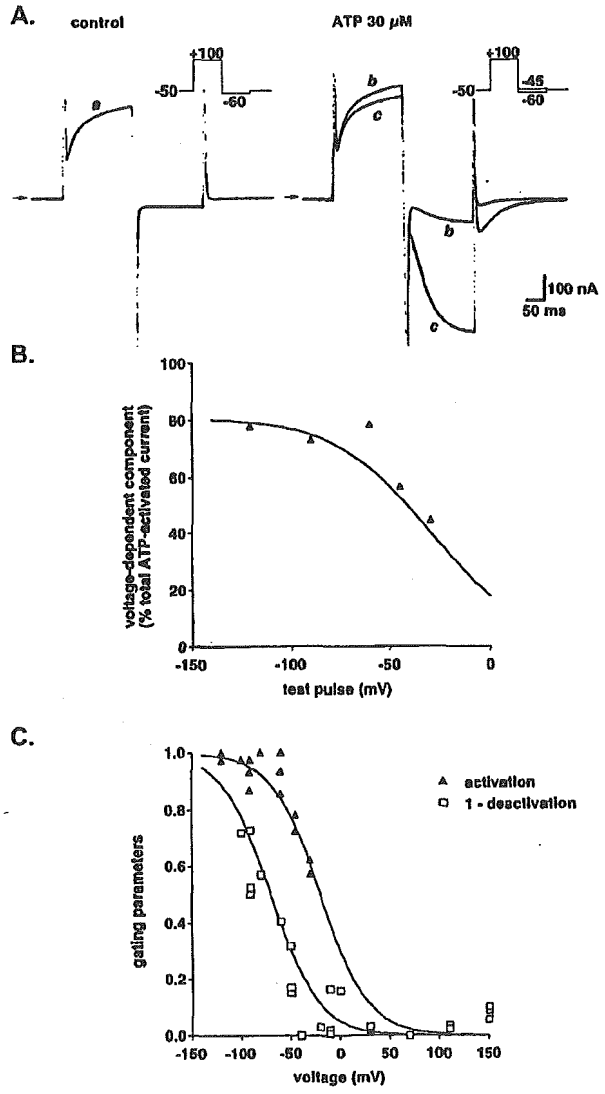

Fig. 7. Effect of hyperpolarization on voltage-dependent current. (A) Current traces before (control) and during the application of 30 μM ATP. In the panel on the right, two current traces obtained following hyperpolarization at −45 mV ("b") and −60 mV ("c") are superimposed. (B) Contribution of voltage-dependent current to total ATP-evoked current at various hyperpolarization potentials. Some of these data are shown in panel A. (C) Comparison of activation and deactivation. Parameters describing activation and deactivation were determined as described in the text. Each data point represents data obtained from individual oocytes.

4. Discussion

4.1. Schematic model of voltage-dependent gating

Recombinant $P2X_2$ receptor/channels expressed in *Xenopus* oocytes exhibited voltage-dependent gating properties similar to those of the channels in PC12 cells (Nakazawa et al., 1997b). The following similarities were observed: (1) the gate opens at negative potentials, (2) activation follows a time course with a time constant of 40 to 70 ms, and (3) gating depends on ATP concentrations. Thus, voltage-dependent gating in PC12 cells may be due to intrinsic expression of $P2X_2$ receptor/channels. We depict here a model that has been proposed to explain voltage-dependent gating of the channels in PC12 cells (Scheme 2):, where A is ATP, R_L and R_H represent closed states, and R* represents the open state (Nakazawa et al., 1997b). In this model, voltage-dependent gating is explained by transition between low and high ATP-affinity states. Upon hyperpolarization, there is a shift from the R_L to the R_H conformation. ATP preferentially binds to channels in the R_H state ($A \cdot R_H$), after which the channels open ($A \cdot R_H^*$). Binding of ATP is the rate-limiting step since activation kinetics were observed to depend on ATP concentrations in the present study (Fig. 3C). The following rate constants have been proposed (Scheme 3): where k_{+1} parallels the concentration of ATP ($k_{+1}=k'_{+1}$[ATP]), and K_d is given by k_{-1}/k'_{+1} (Hille, 1992b). In the present experiment, an activation time constant of 65 ms was observed in the presence of 30 μM of ATP (Fig. 4), which is equivalent to a rate constant of 15 s^{-1}. Using these values, $k'_{+1}=k_{+1}/[ATP]=15\ s^{-1}/(30\ \mu M)=5\times10^5\ M^{-1}\ s^{-1}$. An inactivation time constant of 70 ms was observed in the presence of 30 μM of ATP (Fig. 5), which is equivalent to a rate constant of 14 s^{-1}. Thus, K_d was calculated to be $k_{-1}/k'_{-1}=14\ s^{-1}/(5\times10^5\ M^{-1}\ s^{-1})=28$ μM, which is slightly less than the EC_{50} value obtained at −50 mV (about 40 μM). This estimation is in accordance with the finding that the voltage-dependent component is not completely activated at −50 mV (Fig. 7C). It is difficult to quantify the low-affinity ATP binding state since the relationship between concentration and response needs to be assessed at highly positive potentials, while $P2X_2$ receptor/channels permit only small current due to their inward-rectifying

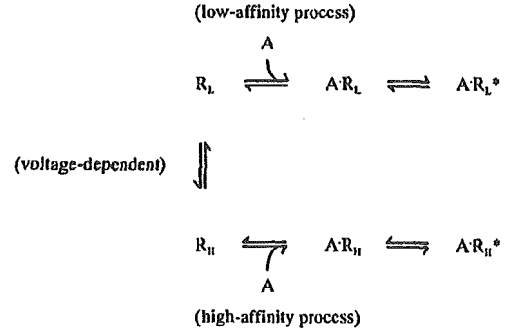

Scheme 2.

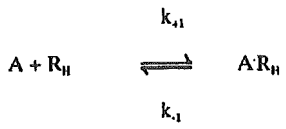

Scheme 3.

nature. We estimate here the low affinity from simple theoretical concentration–response curves. Fig. 8 shows two concentration–response curves. One demonstrates an EC_{50} of 30 μM, corresponding to a high-affinity state. If the other low-affinity state demonstrates an EC_{50} of 100 μM, more $P2X_2$ receptor/channels were in the high-affinity state in the presence of 10 μM ATP, and more were in the low-affinity state in the presence of 300 μM ATP. This is consistent with the greater observed contribution of the voltage-dependent component to total ATP-evoked current in the presence of 10 μM, while little was observed in the presence of 300 μM ATP (Fig. 3). Thus, the low-affinity state may be lower than the high-affinity state by threefold or larger.

The idea of the transition of $P2X_2$ receptor/channels between low- and high-affinity states might explain the "non-voltage-dependent" component of ATP-evoked current. For example, the current evoked by 30 μM ATP was not completely observed as voltage-dependent component even when activated at very negative potentials (Fig. 7B) or following deactivation at very positive potentials (Fig. 6B). This "non-voltage-dependent current" (about 20% of the total ATP-evoked current) might result from the activation of $P2X_2$ receptor/channels in the low-affinity state prior to voltage-dependent activation.

The voltage dependence of activation and deactivation differed, with deactivation occurring at more negative potentials (Fig. 7C). This indicates that the activation and the deactivation do not arise from a simple reversible "back-and-forth" process, rather, two voltage-dependent processes

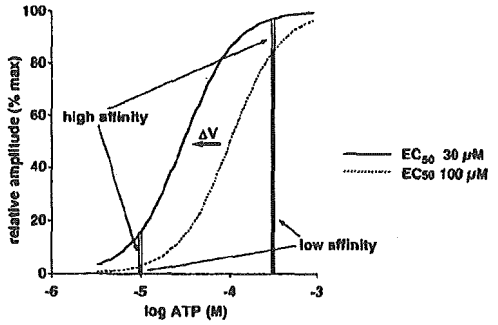

Fig. 8. Voltage-dependent change in sensitivity to ATP might explain dependence of the voltage-dependent current on ATP concentration. Low-affinity (EC_{50}=100 μM) and high-affinity (EC_{50}=30 μM) states of the receptor are thought to exist (Hill coefficient; 1.5). Each receptor shifts from a low-affinity to a high-affinity state upon hyperpolarization (ΔV). With 10 μM ATP, only a small proportion of the receptors, many of which were in the low-affinity state, were activated prior to hyperpolarization, but many more were activated upon induction of the high-affinity state by hyperpolarization. In the presence of 300 μM ATP, a larger proportion of the receptors were activated even in the low-affinity state, and induction of the high-affinity state caused only a marginal increase in activated receptors.